

# **CONCEPTS OF RAINWATER USE FOR THE IRRIGATION OF VERTICAL GREENERY SYSTEMS**

**Master thesis**

**In partial fulfilment of the requirements**

**for the degree of**

**Diplomingenieur**

submitted by:

**PRENNER, FLORA**

Supervisor: Langergraber, Günter, Priv.-Doz. Dipl.-Ing. Dr.nat.techn.

Co-Supervisor: Pucher, Bernhard, Dipl.-Ing.



## ***Acknowledgements***

This thesis was written under the supervision of Priv.-Doz. DI Dr. Günter Langergraber and under the co-supervision of DI Bernhard Pucher at the Institute of Sanitary Engineering and Water Pollution Control at the University of Natural Resources and Life Sciences, Vienna (BOKU). I want to thank Günter for giving me the opportunity to write about this great topic and contribute to the EU-SUGI research project “Vertical Green 2.0”. I further want to thank Bernhard for his time and patience during the past year of working on this thesis. His guidance and helpful discussions have been very valuable.

I want to thank the whole project team of “Vertical Green 2.0” for the great work environment and for giving me insight into the interdisciplinary nature of the topic. I especially want to thank Karin Hoffmann, M.Sc. from TU Berlin and DI Irene Zluwa from the Institute of Soil Bioengineering and Landscape Construction for their helpful expertise and their constructive feedback on my database.

Last but definitely not least, I want to thank my family and friends for their constant support and understanding, their motivational talks and proofreading. It would have been a lot harder without their support!



## **Table of contents**

<b>1. Introduction</b>	<b>1</b>
<b>2. Objectives</b>	<b>3</b>
<b>3. Fundamentals</b>	<b>4</b>
3.1 Vertical Greenery Systems	4
3.1.1 Green facade	4
3.1.2 Continuous living wall	5
3.1.3 Modular living wall	5
3.2 Soil-plant-atmosphere continuum	5
3.2.1 Soil physical basics	5
3.2.2 Water movement	7
3.3 Urban rainwater harvesting	9
3.3.1 General design	9
3.3.2 Rainwater quality and quality requirements	10
<b>4. Material and methods</b>	<b>11</b>
4.1 Conceptual model	11
4.2 VGS database	12
4.2.1 Calculation method	12
4.2.2 Location	13
4.2.3 System design	13
4.2.4 Planting	13
<b>5. Results and discussion</b>	<b>15</b>
5.1 Conceptual model	15
5.1.1 Governing equations	16
5.1.2 Discussion of conceptual model	20
5.1.3 VGS boundary conditions	22
5.1.4 RWH scenarios	23
5.2 VGS database	24
5.2.1 Analysis of water demand and irrigation amounts	24
5.2.2 Analysis of VGS characteristics	33
5.2.3 Discussion of database results	38
<b>6. Conclusions</b>	<b>43</b>
<b>7. Summary and outlook</b>	<b>45</b>
<b>8. References</b>	<b>47</b>
<b>9. Appendix</b>	<b>51</b>
9.1 Details VGS database	51
9.2 Water demand and irrigation amounts	57
<b>10. Curriculum Vitae</b>	<b>58</b>
<b>11. Affirmation</b>	<b>60</b>



## List of figures

Figure 1: Global land and ocean temperature anomalies 1880 – 2019 (NOAA National Centers for Environmental Information State of the Climate, 2019).....	1
Figure 2: Visualization of VGS benefits (adapted from Pfoser <i>et al.</i> , 2013).....	2
Figure 3: Examples of different VGS types (Bustami <i>et al.</i> , 2018). ....	4
Figure 4: Soil water retention curve (adapted from Amelung <i>et al.</i> , 2018).....	7
Figure 5: Areal view of urban structure with a) low degree of development and building density, and b) high degree of development and building density (Simperler <i>et al.</i> , 2018). ....	12
Figure 6: Conceptual model. ....	15
Figure 7: Annual total water demand and irrigation amounts (marked with a star) per m <sup>2</sup> for continuous living walls (yellow), green facades (green) and modular living walls (blue).....	27
Figure 8: Annual water demand and irrigation amounts (marked with a star) per m <sup>2</sup> for continuous living walls (yellow), green facades (green) and modular living walls (blue).....	28
Figure 9: Annual water demand and irrigation amounts (marked with a star) per m <sup>2</sup> for continuous living walls (yellow), green facades (green) and modular living walls (blue). Without Mexico_VGS. ....	30
Figure 10: Daily water demand and irrigation amounts (marked with a star) per square meter greened area for continuous living walls (yellow), green facades (green) and modular living walls (blue).....	31
Figure 11: Daily water demand and irrigation amounts (marked with a star) per kilogram biomass on a summer day for continuous living walls (yellow) and modular living walls (blue). ....	32
Figure 12: Daily water demand and irrigation amounts (marked with a star) per substrate volume on a summer day for continuous living walls (yellow), green facades (green) and modular living walls (blue). ....	33
Figure 13: Total substrate volume plotted against the water demand/irrigation amount per square meter greened area on a summer day for continuous living walls (yellow), green facades (green) and modular living walls (blue). Left: without Mexico_VGS, right: without Mexico_VGS and MA31. ....	34
Figure 14: Water demand/irrigation amounts (*) per m <sup>2</sup> and relative substrate volume of modular living walls with (left) and without (right) MA31. ....	35
Figure 15: Water demand/irrigation amounts (*) per m <sup>2</sup> and relative substrate volume of continuous living walls without Mexico_VGS. ....	35
Figure 16: Relative biomass plotted against the daily water demand and irrigation amounts per kilogram biomass for a summer day for continuous living walls (yellow) and modular living walls (blue) with (left) and without (right) MA31. ....	36
Figure 17: Greened area plotted against the water demand/irrigation amount for a summer day for continuous living walls (yellow), green facades (green) and modular living walls (blue) with (left) and without (right) MA31. ....	37
Figure 18: Total greened area in square meters for continuous living walls (yellow), green facades (green) and modular living walls (blue). ....	38
Figure 19: Comparison of the water demand per square meter for SiteC_Berlin, calculated with the course of the greened area (green) and with a constant greened area of 25 m <sup>2</sup> (grey).....	39
Figure 20: Conceptual model.....	45

## **List of tables**

Table 1: VGS Kc values from literature for Penman-Monteith modelling of ET. ....	21
Table 2: Analysed VGS, type and data available for irrigation demand analysis. ....	25
Table 3: Köppen-Geiger climate types and general climate classifications after Peel <i>et al.</i> (2007). DfB = Warm-summer humid continental climate; Csa = Mediterranean hot summer climate; Cfb = Oceanic climate; BSh = Semi-arid climate. ....	29
Table 4: Comparison of substrate characteristics and water demand of selected sites. ....	34
Table 5: Available information in the database. ....	40
Table 6: Greened area, relative substrate volume and relative biomass of the VGS investigated. .....	41
Table 7: General data and location information of the VGS investigated. ....	51
Table 8: System design of the VGS investigated. ....	52
Table 9: Part 1 – Planting of the VGS investigated. ....	53
Table 10: Part 2 – Planting of the VGS investigated. ....	54
Table 11: Part 1 – Water supply of the VGS investigated. ....	55
Table 12: Part 2 – Water supply of the VGS investigated. ....	56
Table 13: Water demand and irrigation amounts (*) per month ( $\text{m}^3\cdot\text{month}^{-1}$ ) and annual sum ( $\text{m}^3\cdot\text{year}^{-1}$ ). ....	57



## **Abstract**

Climate change and urbanisation are the two main challenges for modern cities. Vertical greenery systems (VGS) are one possible adaption measure to counteract the effects of climate change on the urban environment. The positive effect of VGS is highly depend on the vegetation. Therefore, VGS need to be irrigated efficiently to ensure healthy plant growth. To reduce the pressure on drinking water resources, alternative water resources must be used for irrigation. This thesis aims at investigating the water demand of VGS and how this demand can be covered with rainwater harvesting (RWH). The methods used for the analysis of VGS water demand are a conceptual model and a VGS database. The water supply from RWH is described using two scenarios, developed for urban environments with a high and a low urban density. The conceptual model shows that the main processes to describe the irrigation demand of VGS are precipitation, evapotranspiration, run-on, percolation and overflow. The governing equations for the calculation of the water demand and the boundary conditions for three VGS types are presented in this thesis. The results of the database analysis show that continuous living walls have a higher annual water demand per square meter compared to modular living walls and green facades. The water demand can be covered by harvesting rainwater from streets and roofs. In low density areas, this demand is recommended to be covered by harvesting rainwater from roofs and installing a RWH system on the building scale. In high density areas, it is suggested to harvest run-off from roof and/or street surfaces and install the RWH system on a building scale or on a block scale. Further detailed analyses of VGS water demand are required to allow a targeted use of VGS for mitigating the effects of climate change on the urban environment.

## **Zusammenfassung**

Klimawandel und Urbanisierung sind zwei der größten Herausforderungen für moderne Städte. Vertikale Begrünungssysteme (VGS) sind eine mögliche Maßnahme, um den Auswirkungen des Klimawandels in Städten entgegenzuwirken. Der positive Effekt von VGS hängt stark von der Vegetation ab. VGS müssen effizient bewässert werden, um ein gesundes Pflanzenwachstum sicherzustellen. Um den Druck auf Trinkwasserressourcen zu verringern, müssen alternative Wasserressourcen für die Bewässerung genutzt werden. Diese Arbeit untersucht den Wasserbedarf von VGS und wie dieser Bedarf durch Regenwassernutzung (RWH) gedeckt werden kann. Für die Analyse des Wasserbedarfs wurden ein konzeptionelles Modell und eine VGS-Datenbank erstellt. Die Wasserversorgung mit gesammeltem Regenwasser wurde anhand von zwei Szenarien, für ein Gebiet mit hoher und ein Gebiet mit niedriger Dichte, beschrieben. Das konzeptuelle Modell zeigt, dass sich der Bewässerungsbedarf von VGS hauptsächlich aus Niederschlag, Evapotranspiration, Oberflächenzulauf, Versickerung und Überlauf zusammensetzt. Die Formeln für die Berechnung des Wasserbedarfs und die Randbedingungen für die drei VGS-Typen werden in dieser Arbeit vorgestellt. Die Auswertung der Datenbank zeigt, dass "continuous living walls" einen höheren jährlichen Wasserbedarf pro Quadratmeter begrünter Fläche haben als "modular living walls" und Grünfassaden. In Gebieten mit geringer Bebauungsdichte wird empfohlen, diesen Wasserbedarf mit Abfluss von Dächern zu decken und das RWH System im Gebäude zu installieren. In Gebieten mit hoher Dichte kann der Wasserbedarf mit einer Kombination aus Dach- und Straßenabfluss gedeckt werden. Es wird empfohlen das RWH System im Gebäude oder im Häuserblock zu platzieren. Es bedarf jedoch weiterer Forschung des VGS-Wasserbedarfs, um einen gezielten Einsatz von VGS zur Minderung der Auswirkungen des Klimawandels auf die städtische Umwelt zu ermöglichen.



## Abbreviations

CO <sub>2</sub>	Carbon dioxide
CR	Capillary rise
ET	Evapotranspiration
ET <sub>0</sub>	Reference evapotranspiration
ET <sub>c</sub>	Evapotranspiration under standard conditions
ET <sub>c adj</sub>	Evapotranspiration under non-standard conditions
FC	Field capacity
K <sub>c</sub>	Crop coefficient
NBS	Nature-based solution
$k_{sat}$	Saturated hydraulic conductivity
$k_{unsat}$	Unsaturated hydraulic conductivity
LA	Leaf area
PM	FAO-56 Penman-Monteith
PWP	Permanent wilting point
RC	Run-off coefficient
RWH	Rainwater harvesting
SWMM	Storm Water Management Model
UHI	Urban Heat Island
VGS	Vertical greenery systems
WA	Wall area
WLAI	Wall leaf area index
WUCOLS	Water Use Classifications of Landscape Species



# 1. Introduction

The global climate change results in rising temperatures. The anomalies in temperature are increasing steadily in the last decades, as shown in Figure 1 (NOAA National Centers for Environmental Information State of the Climate, 2019). Increasing temperatures lead to discomfort and economic losses, can be the driver of migration movements and raise mortality rates (Haines *et al.*, 2006). Moreover, the changing temperatures impact the local weather and result in more frequent extreme weather events. Heat and cold waves, floods, droughts, wildfires and windstorms are predicted to increase (Forzieri *et al.*, 2016). Consequently, the effects of climate change strongly influence the environment and people's day to day lives.

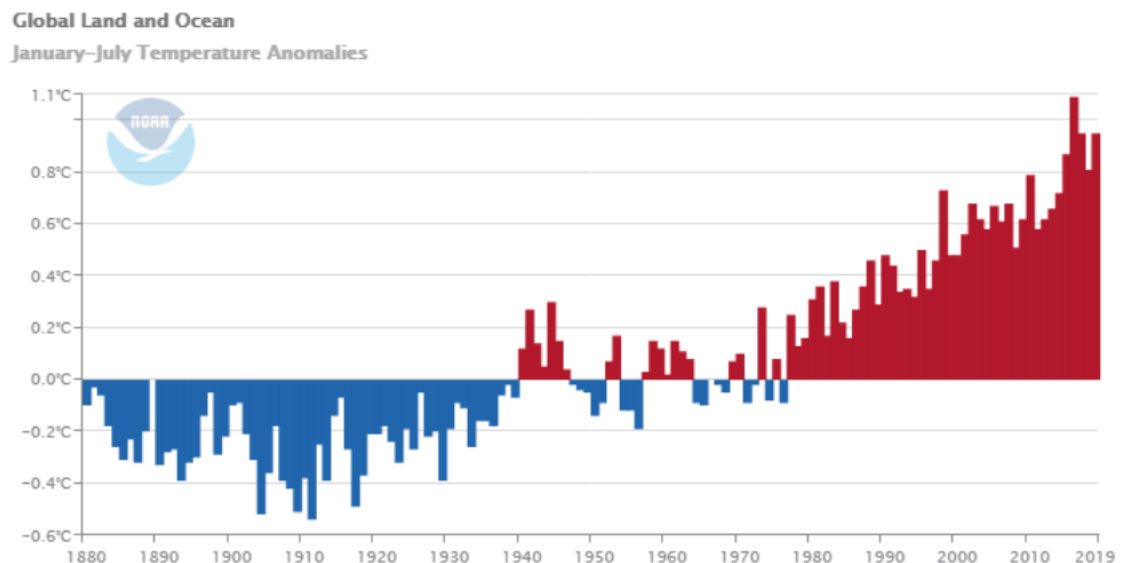


Figure 1: Global land and ocean temperature anomalies 1880-2019 (NOAA National Centers for Environmental Information State of the Climate, 2019).

At the same time, a global urbanisation process can be observed. By 2050, approximately 68% of the world's population are projected to live in cities (United Nations, 2018). Urban densification allows a more efficient use of land and resources, and can therefore act as a sustainable development measure (Emilsson and Ode Sang, 2017). However, urbanisation comes along with changes in land cover and use, alterations of the hydrologic system, impacts on biodiversity, influences on the biogeochemical cycle and changes in local climate. Amongst others, the resulting problems are an increase of sealed surfaces, an accumulation of pollutants in streams, an increase of carbon dioxide (CO<sub>2</sub>) and greenhouse gas emissions, raising temperatures, a reduced species richness and evenness (Grimm *et al.*, 2008). The increase in local temperatures is also known as the urban heat island effect (UHI). Temperatures in cities are rising due to "increased impervious surfaces (low albedo, high heat capacity), reduced areas covered by vegetation and water (reduced heat loss due to evaporative cooling), increased surface areas for absorbing solar energy due to multi-storey buildings, and canyon-like heat-trapping morphology of high-rises" (Grimm *et al.*, 2008).

These two processes – climate change and urbanisation – are the main challenges for modern cities. As cities are generally more susceptible to pollution, higher temperatures, more rain and less wind than rural surroundings (Givoni, 1991), the effects of climate change will be even enhanced. Rising temperatures will intensify the UHI effect and extreme storm events will challenge the capacity of the channelled, urban drainage systems (Emilsson and Ode Sang, 2017; Semadeni-Davies *et al.*, 2008). Measures are needed to not only mitigate but adapt to the effects of climate change. These adaption measures can ensure long-term strategies "to reduce the vulnerability of society and to improve the resilience capacity against expected changing climate" (Depietri and McPhearson, 2017; Emilsson and Ode Sang, 2017). Adaption measures

can be implemented in many forms. Depietri and McPhearson (2017) distinguish between grey, green and blue, and hybrid measures. Grey measures are made of concrete and include dikes, stormwater sewers and air conditioning. Green and blue measures are healthy ecosystems with light management, such as forests, parks, street trees and wetlands. Hybrid measures are engineered ecosystems and combine the two previous measures. Examples for hybrid systems are raingardens, green roofs and restored wetlands.

Nature based solutions (NBS) are adaption measures, which use natural processes to reduce the effects of climate change on the urban environment. The European Commission (EC DG, 2015) defines NBS as “living solutions inspired by, continuously supported by and using nature, which are designed to address various societal challenges in a resource-efficient and adaptable manner and to provide simultaneously economic, social, and environmental benefits”. Vegetation plays a crucial role in the contribution of NBS to ecosystem services. Their evapotranspiration process regulates the surrounding microclimate by contributing to a higher humidity and lower temperatures (Enzi *et al.*, 2017). In cities, horizontal areas on street level are often occupied by infrastructure such as streets or parking spaces. This limits the implementation possibilities of NBS. However, the building roof and the vertical facade area offer great potential for the implementation of adaption measures (Köhler, 2008). Building greenings include Vertical Greenery Systems (VGS) and green roofs, whereas this thesis is focusing on VGS only. VGS are greening the building facades by growing plants vertically (Bustami *et al.*, 2018). The main ecosystem services provided by VGS include a) reduction in temperature, b) improvement of air quality, c) noise reduction, d) additional building insulation and e) increase of biodiversity (compare Figure 2). Furthermore, greenery improves the aesthetic of cities and has proven to positively impact people’s psychological wellbeing (Manso and Castro-Gomes, 2015).

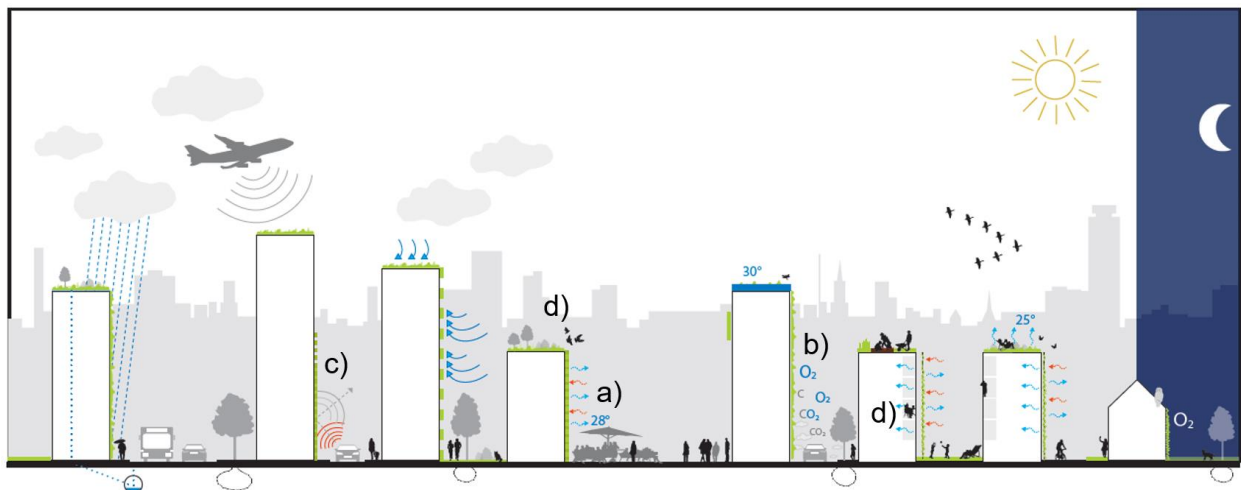


Figure 2: Visualization of VGS benefits (adapted from Pfoser *et al.*, 2013).

To provide those benefits, the well-being of the plants in VGS must be ensured. Irrigation is a key factor for healthy plant growth. However, irrigation water demand should not compromise drinking water resources. Hence, irrigation should be optimally designed to reduce losses and water should come from sustainable sources such as rainwater. Rainwater harvesting (RWH) is a possible source of irrigation water, using the run-off from sealed surfaces. Thereby, RWH is contributing to a reduction of run-off load diverted to the sewer system and helps to reduce the pressure of flooding within the city (Farreny *et al.*, 2011).

This thesis aims at investigating the water demand of VGS and how this demand can be satisfied with rainwater. In the period from March 2019 to January 2020, a conceptual model and a VGS database was created to get new insights into the sustainable implementation of VGS. The work was carried out within the "Urban Vertical Greening 2.0" project, which aims at identifying the different chances and challenges associated to VGS in order to maximize their acceptance (Vertical Green 2.0, 2018). The outcomes of this thesis support future implementation projects of VGS to make them an integral part of modern city and building planning and design.

## 2. Objectives

This thesis aims at creating a conceptual model of VGS to understand the surface-plant-air interactions in VGS and further be able to calculate their water demand. This supports the prediction of the optimal irrigation amount. In additional, the model aims at describing possible scenarios for the irrigation of VGS with harvested rainwater.

To achieve these objectives, the following research questions are examined:

- 1) How can the optimal water demand of a Vertical Greenery System be calculated?
- 2) How can this demand be provided from rainwater collection?

The following tasks are defined in order to fulfil the above-mentioned objectives:

- Create a conceptual model to visualize the hydrological processes and VGS elements
  - Define the governing equations to calculate the water demand
  - Describe the boundary conditions of the different VGS types
  - Describe the RWH scenarios for two different urban structure types
- Create a VGS database of existing greeneries
  - Gather data on water and irrigation, location, system design and planting
  - Compare the water and irrigation demands
  - Analyse the influence of system properties on the water demand

The thesis is structured in three main chapters: Fundamentals, material and methods, and results and discussion.

The subsequent chapter describes the fundamentals needed to answer the research questions. First, VGS are described and the different VGS types are presented. This is followed by a description of the soil-plant atmosphere continuum to get a better understanding of the hydrological processes in VGS. Finally, the characteristics of urban rainwater harvesting are presented.

In Chapter 4, materials and methods used to create the conceptual model and the VGS database are explained. The calculation methods used for the database and parameters collected for the analysis of water and irrigation amount are described.

The obtained conceptual model and the database are presented and discussed in Chapter 5.

In Chapter 6, the thesis closes with a conclusion and outlook to future research.

### 3. Fundamentals

#### 3.1 Vertical Greenery Systems

VGS are systems with “plants grown on a vertical profile” (Bustami et al., 2018) and can be subdivided in green facades (Figure 3a) and living walls (Figure 3b). Living walls can further be classified as continuous or modular, depending on the use of a growing medium. VGS design is based on the following system components: Supporting elements, growing media, vegetation, irrigation and drainage (Manso and Castro-Gomes, 2015).

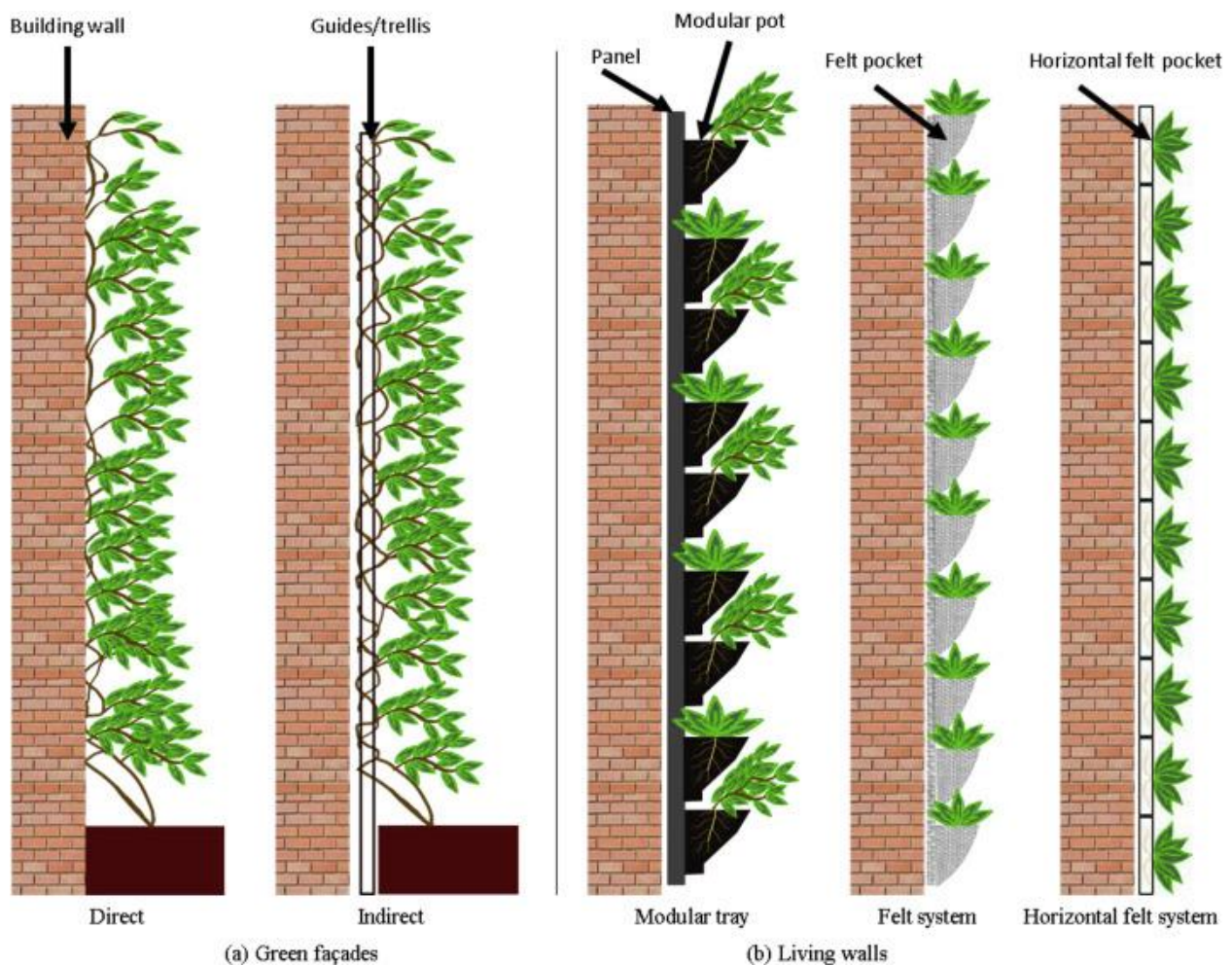


Figure 3: Examples of different VGS types (Bustami *et al.*, 2018).

##### 3.1.1 Green facade

Green facades can either be directly grown on the facade or indirectly grown along a vertical support adjoined to a building facade. This vertical support avoids putting additional weight on the facade and can be in the form of cables, ropes, nets or trellises made of different materials. The growing medium can either be ground soil or substrate in vessels. The vessels can be positioned on ground level or hung at a certain height. For planting, climbing plants are used to ensure a covering of the building facade. When grown directly in the ground, the substrate is the natural soil and excess water is drained naturally into the soil. If the plants are grown in vessels, drainage has to be ensured by holes to avoid waterlogging. When grown directly in the ground, irrigation water can either come from street run-off or drip line irrigation. For vessel grown green facades, mainly drip irrigation is used (Manso and Castro-Gomes, 2015).



### 3.1.2 Continuous living wall

Continuous living walls do not rely on rooting space on the ground as the plants are grown in lightweight and permeable screens. They are supported by a frame attached to the wall that holds the base panel and the “permeable, flexible and root proof screens” (Manso and Castro-Gomes, 2015). On the outside, the last layer is cut open to form pockets where the plants can be inserted. Continuous living walls do not use potting soil as substrate, but artificial materials such as mineral wool or fleece (Pitha *et al.*, 2013). As the capillary rise of mineral wool is quite low, continuous living walls are designed as hydroponic systems. Therefore, a constant supply of nutrients and water is necessary to ensure a good plant development (Manso and Castro-Gomes, 2015; Van de Wouw *et al.*, 2017). Drainage is facilitated by an extra geotextile along the permeable membrane. Continuous living walls are irrigated by drip irrigation installed on different heights. The distribution of water and nutrients is ensured by the permeable screen (Manso and Castro-Gomes, 2015).

### 3.1.3 Modular living wall

Modular living walls use various containers such as trays, vessels, planter tiles or flexible textile bags attached to the facade. Several boxes can be combined to modules, which again are interlocked with each other. The substrate is a mixture of organic and inorganic material. To reduce weight, inorganic components such as foam particles can be added. To ensure a good water retention and further reduce weight, the growing material typically contains porous or expanded material like coconut fibres or mineral granules. Also, drainage is enhanced by adding coarse granular material (e.g. expanded clay, expanded slate, gravel) to the bottom of the modules. Drainage can be further improved through a specific design of the plant containers. Container bottoms with inclination, perforation or concavity help to avoid waterlogging. The overlapping modules allow the reuse of drainage water from higher levels for the irrigation of the modules below. Similar to the irrigation of a continuous living wall, modular living walls are mostly irrigated by drip irrigation (Manso and Castro-Gomes, 2015).

## 3.2 Soil-plant-atmosphere continuum

### 3.2.1 Soil physical basics

Soil water is bound by various forces, so different types of water bindings exist. In part, soil water can move freely through the matrix, however, partially the water is bound to the matrix. Gravity water is not held by the soil matrix against gravitational forces and moves freely through the soil matrix. It can be collected above a layer with low permeability or low hydraulic conductivity, forming a groundwater storage. However, hygroscopic and capillary water can be held against the gravitational forces. Hygroscopic water covers the soil particles and is held by adsorptive and osmotic forces. The amount of adsorption water rises with an increasing relative water vapour pressure of the surrounding air and with decreasing particle size. The capillary water is held in the soil matrix by adhesion (between solid and liquid surfaces) and cohesion (between water molecules) forces. Due to the tendency of a minimal boundary surface between water and air, menisci are formed. The smaller the pore diameter (like in silty and loamy soils), the stronger the capillary water is bound (Amelung *et al.*, 2018; Dingman, 2015).

The soil water potential influences the water movement in the soil. The total soil water potential is defined as “the amount of useful work per unit mass of pure water, that must be done by means of externally applied forces to transfer reversibly and isothermally an infinitesimal amount of water from the standard state  $S_0$  to the soil liquid phase at the point under consideration” (International Society of Soil Science, 1952). Water always moves along a potential gradient from a higher to a lower potential. The water movement is stopped as soon as the total potential is in an equilibrium in all points of the soil matrix. The units in the following equations are standardised by using L as the unit of length, T as the unit of time, M is the unit of mass and  $\theta$  is the unit of temperature. The total water potential  $\psi_t$  is defined as,

$$\psi_t = +\psi_g - \psi_o - \psi_m \quad (1)$$

where:

$\psi_g$  is the gravitational potential (L);

$\psi_o$  is the osmotic potential (L); and

$\psi_m$  is the matric potential (L).

The gravitational potential  $\psi_g$  is the required work to lift water from the standard system  $S_0$  against gravity to a certain height. The reference height for  $\psi_g$  is the water table and increases with increasing distance to the water table. The osmotic potential  $\psi_o$  is the required work to extract water from a solution through a semipermeable membrane.  $\psi_o$  is included as soil water is never only pure water, but a solution with soluble salts. The matric potential  $\psi_m$  expresses the influence of the soil matrix on the water movement.  $\psi_m$  is the required work to extract water from a soil pore against the capillary forces (Amelung *et al.*, 2018).

The hydraulic conductivity  $k$  (L.T<sup>-1</sup>) is a soil characteristic describing the water permeability of a soil.  $k$  is significantly influenced by the amount, size and form of the soil pores: generally, bigger pore diameters result in a higher  $k$  value. In the saturated zone,  $k$  is constant as all pores are filled with water, whereas macropores contain the most water. If the soil drains, the water from these macropores drains first and leaves air cavities. So under unsaturated conditions the pores are filled with water and air. The resulting air cavities reduce the water flow.  $k$  in the unsaturated zone is therefore a function of water content and water tension. With a decreasing water content,  $k$  decreases as well (Amelung *et al.*, 2018).

For a given soil, there is a relationship between the matric potential and the water content. A soil water retention curve can be drawn, showing the function  $h(\theta)$  graphically and giving indications about the water holding capacity of a soil (Figure 4). The graph shows the water content at a specific matric potential. The course of the relationship between the two is characteristic for every soil, as it is dependent on pore volume and pore size distribution. The water content at saturation is the water content at a matric potential of 0 hPa. Furthermore, the graph shows the water content in the range of the plant available water, which is relevant for irrigation purposes (Amelung *et al.*, 2018).

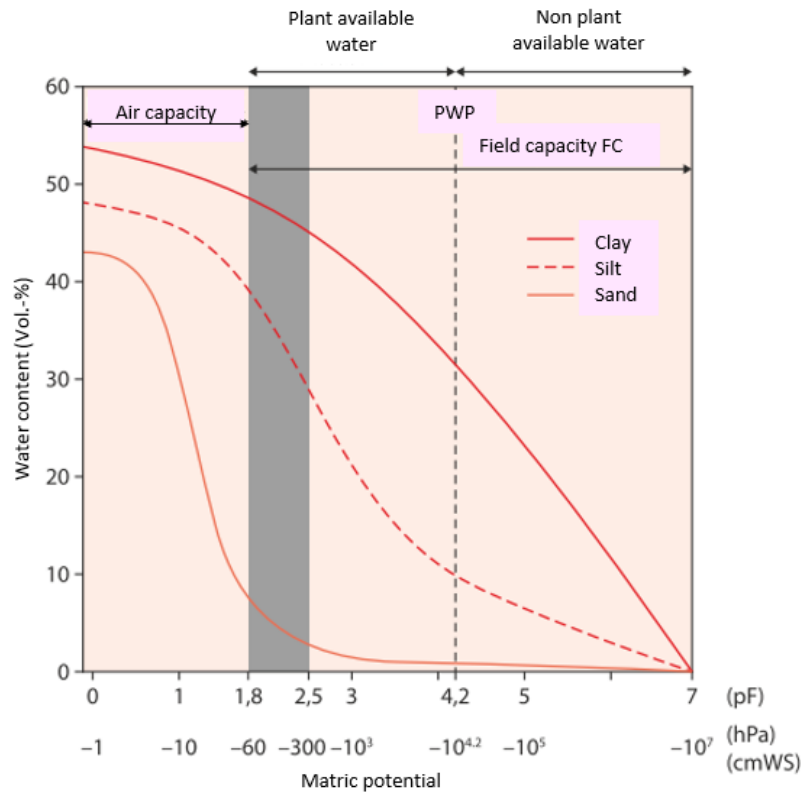


Figure 4: Soil water retention curve (adapted from Amelung *et al.*, 2018).

More specifically, the course of the curve is influenced by 1) the soil texture, 2) the soil structure and 3) the hysteresis effect. 1) The soil texture represents the proportion of sand, silt and clay particles in a soil and the resulting pore volume. Soils with a bigger share of coarse pores (such as sandy soils) have a lower water retention capacity, than soils with a bigger share of middle and fine pores (such as silty and loamy soils). Additionally, silty and loamy soils have a higher share of clay particles, which have a bigger adsorbing surface area. 2) The soil structure is the arrangement of particles and pores in the soil. The structure influences the water retention capacity especially in shrinking and swelling clay soils, which changes the pore size distribution. 3) The hysteresis effect is the change of the soil water retention content curve with irrigation and drainage of the soil. Shrinking and swelling lead to changes in the soil structure and therefore change the water retention curve.

For every soil, there are specific water content measures: the field capacity (FC) and the permanent wilting point (PWP). Dingman (2015) defines the FC as “the water-content at which the gravity-drainage rate becomes ‘negligible’”. Usually, FC is reached 1-2 days of free drainage after saturation and is therefore the soil water content, which can be held against gravity forces. PWP is the soil water content at which plants show signs of wilting and are permanently harmed, as the transpiration amount cannot be replaced by water from the soil. The PWP is generally considered to be the water content at a matric potential of 15000 hPa (Dingman, 2015).

### 3.2.2 Water movement

The water movement in the soil is driven by the soil water potential gradient and is limited by the hydraulic conductivity. The water movement is explained by Darcy’s law of water flow through a porous medium from 1856:

$$q = -k_{sat} * \frac{d\psi}{dl} \quad (2)$$

where:

$q$  is the specific discharge ( $L \cdot T^{-1}$ );

$k_{sat}$  is the saturated hydraulic conductivity ( $L \cdot T^{-1}$ ); and

$\frac{d\psi}{dl}$  is the gradient of the total hydraulic head (-).

The general equation for the saturated and unsaturated flow is based on Darcy's law in combination with the continuity equation. In case of unsaturated flow,  $k$  is a function of the water content. As subsurface flow is mostly nonstationary due to the water content changes, the sum of the equation is the change in water content over time. For vertical downward flow, this is combined in the Richard's equation, often used for modelling infiltration and redistribution:

$$\frac{\partial \theta}{\partial t} = \frac{\partial}{\partial z} \left[ k \left( \frac{\partial \psi}{\partial z} + 1 \right) \right] \quad (3)$$

where:

$\frac{\partial \theta}{\partial t}$  is the change in water content over time ( $T^{-1}$ ); and

$\frac{\partial \psi}{\partial z}$  is the gradient of the matric head in z-direction (-).

The value “+1” ensures that the gravitational influence in the vertical flow is included. In z-direction  $\frac{\partial \psi_z}{\partial z}$  equals 1, therefore only the term  $\partial k$  is left from the Darcy equation (Amelung *et al.*, 2018; Dingman, 2015).

The water flow in the medium is especially important for effective irrigation, as it determines the distribution of the water in the substrate. The water distribution in the substrate affects plant water uptake, evaporation and the preferential pathways of new irrigation water (Prodanovic *et al.*, 2019)

Infiltration is the movement of water from the surface into the soil. It follows precipitation, irrigation or ponding and results in a less negative matrix potential at the surface than in the equilibrium state. A vertical movement downwards is started. The course of infiltration is given by the infiltration rate (Amelung *et al.*, 2018). There are three possible infiltration conditions: 1) no ponding occurs and the “infiltration rate equals the water-input rate”, 2) ponding occurs because the “water input rate exceeds the infiltration rate”, which is defined by the soil type and wetness, or 3) ponding occurs because the soil is saturated (Dingman, 2015).

Evaporation describes the process of liquid water being transformed to water vapour. The driving force for evaporation is the incoming radiation. Water molecules can only leave their liquid state, if the vapour pressure of the air layer above the liquid is below saturation vapour pressure. Saturation vapour pressure is the maximum vapour pressure at the present temperature. With an increasing surface temperature, the saturation vapour pressure increases, and more molecules can leave the liquid. Air movement helps to distribute the vapour molecules above the surface. If the water molecules gather and the vapour pressure in the thin air layer above the liquid surface reaches the saturation vapour pressure at surface temperature, no additional evaporation can occur (Dingman, 2015).

Evaporation results in a lower matrix potential at the soil surface. As described before, water movement always occurs from places with higher, to places with lower potential. Therefore, evaporation results in a soil water movement directed upwards (Amelung *et al.*, 2018).

Transpiration is the process of water evaporating from the stomatal cavities of plants. This water movement is induced by a vapour-pressure difference between the cavities and the atmosphere, which entails a potential-energy gradient in the whole plant. This gradient is responsible for root water uptake from the soil and the translocation of liquid and nutrients through the whole plant. The plants have physiological control over the amount of evaporation via the size of the stomatal openings. The size of the openings is mainly adjusted to the surrounding conditions of light, humidity and water content of the leaf cells, as well as to wind, CO<sub>2</sub>-level and temperature.

Transpiration increases with increasing leaf-area, which leads to a characteristic distribution of transpiration rates throughout the vegetation period (Allen *et al.*, 1998).

As evaporation and transpiration are difficult to measure separately, usually the total evapotranspiration (ET) is measured and modelled. According to the definition of Allen *et al.* (1998), distinctions are made between the reference ET (ET<sub>o</sub>, also called potential ET), the ET under standard conditions (ET<sub>c</sub>) and the ET under non-standard conditions (ET<sub>c adj</sub>). ET<sub>c adj</sub> is the ET under non-optimal conditions as induced by diseases, salinity or water shortage, and the calculation includes additional stress coefficients.

Research conducted for VGS in Melbourne, Australia, shows that higher temperatures are likely to increase ET rates. However, it is difficult to state to which part this is due to a higher evaporation rate or higher transpiration rates (resulting from bigger plant biomass or a stimulated transpiration activity). Furthermore, no correlation between ET and relative humidity was found (Prodanovic *et al.*, 2019).

Capillary rise (CR) is induced by a more negative matrix potential above the groundwater or any other water storage in the substrate body. This potential gradient is due to water evaporating at the soil surface or due to water uptake from plants. The height of the capillary rise is influenced by soil parameters, such as the radius of the soil particles. The height can be calculated with:

$$h_{cr} = \frac{2 * \sigma * \cos(\beta_c)}{\gamma * r} \quad (4)$$

where:

$h_{cr}$  is the column height (L);

$\sigma$  is the surface tension (M.T<sup>-2</sup>);

$\beta_c$  is the contact angle (-);

$\gamma$  is the weight density of water (M.L<sup>-3</sup>); and

$r$  is the average radius of the soil particles (L) (Amelung *et al.*, 2018; Dingman, 2015).

Interception is the share of precipitation falling on the vegetation surface, from where it evaporates. These interception losses are influenced by vegetation (density, type, stage of development) and precipitation (intensity, duration, frequency). The total interception loss from an area includes the canopy and the litter interception loss (Dingman, 2015).

### 3.3 Urban rainwater harvesting

#### 3.3.1 General design

RWH systems can be divided into passive and active systems. Passive RWH systems direct rainwater through overland flow for e.g. crop irrigation. Active RWH systems collect rainwater from impermeable surfaces for indoor and outdoor uses like irrigation, toilet flushing or cooling. This thesis focuses on active RWH systems from sealed areas (Sojka *et al.*, 2016).

RWH systems consists of four functional elements, namely collection, treatment, storage and distribution (ÖNORM EN 16941-1, 2018). Active RWH systems can be divided into gravity-, pumped- and composite systems. Gravity systems are designed with an elevated storage tank, which allows a gravitational rainwater collection and distribution. Design constraints are the load-bearing capacity of the building to carry the additional weight of an elevated tank, and the ability to provide enough water quantity and pressure at the elevated tank. In addition, the operation pressure and the water temperature in the storage might be limitations. Pumped RWH systems are more common. The storage tanks are situated at ground level or underground from where the water is distributed either to another header tank, located at a high point of the building, or directly to the users. Composite systems combine the two approaches to reduce the amount of pumping

needed. The composite RWH consist of a header tank fed by gravity, and a main tank at ground level for excess run-off and run-off from lower surfaces. In case the header tank is empty, water is pumped from the main tank (Woods Ballard *et al.*, 2015).

The position and choice of the RWH system depends on the dimensions and maintenance requirements of the tank and the physical constraints of the location. Generally, tanks should be located in a safe place that can be accessed easily for maintenance work. Underground tanks have proven to perform better in regards of water temperature, bacterial growth and freezing in cold climates. If the tank is installed underground, spatial limitations due to underground facilities (especially in dense urban areas), the groundwater level (to avoid flotation of empty tanks) and the ground composition, should be considered additionally (Woods Ballard *et al.*, 2015).

### 3.3.2 Rainwater quality and quality requirements

The quality of rainwater changes drastically with the type of surfaces the run-off is collected from. Generally, run-off from roofs is less polluted than run-off from street surfaces. The origin of the pollutants is not only resulting from the use or the material specifications of the surface, but also from atmospheric pollution. Additional pollution can occur due to locally specific pollution, such as animal excrements (ÖWAV-Regelblatt 45, 2015). A list of pollutants and their sources can be found for example in Ertl *et al.* (2016), Abbasi and Abbasi (2011) or ÖWAV-Regelblatt 35 (2019). On traffic surfaces, the pollution level is highly dependent on the amount of parking spaces and the changing frequency of cars (ÖWAV-Regelblatt 45, 2015).

The water quality requirements for service water are given in literature. In a brochure, the Senatsverwaltung für Stadtentwicklung Berlin (2007) state that the treated water should be nearly free of suspended matter, nearly odourless, colourless and clear. The oxygen saturation should be preferably above 50% percent to ensure its storability. The Biological Oxygen Demand (BOD<sub>7</sub>) should be below 5 mg/l. The water should be in hygienically and microbiologically perfect condition. Values for bacteriological monitoring can be found in Senatsverwaltung für Stadtentwicklung Berlin (2007 and Environment Agency (2010). Matzinger *et al.* (2017) suggest the EU Bathing Directive (EU, 2006) as a reference for the hygienic requirements of the harvested rainwater intended for service water use.

## 4. Material and methods

### 4.1 Conceptual model

The method used in this thesis to calculate the water demand of VGS and the available water from RWH is a conceptual model based on the specific water balance of VGS. The conceptual model describes the hydrological processes involved in VGS and RWH. To identify these processes a literature research was carried out using the databases of Scopus, Google Scholar and the literature research site of the University of Natural Resources and Life Sciences, Vienna. The research languages were English and German.

First, the literature research aimed at determining the processes describing the water demand of VGS and water supply from RWH. The main processes involved are precipitation, evapotranspiration, run-on, percolation and overflow. These processes were visualized in the conceptual model following the example of the hydrological model by Herrera *et al.* (2017). In a second step, a literature research aimed at collecting equations to quantify the processes and the available water from RWH was performed. The research was focused on finding equations, which were already applied in models on a similar scale as VGS. Therefore, the keywords used in the research were not only related to VGS, but also included green roof modelling.

After the general model was developed, the boundary conditions were described to allow the calculation of the water demand for all three VGS types. Based on the characteristics of the VGS types found through literature research, the possible water inflows and outflows, resulting from differences in the system design, were identified. These specifications are described in the formulas of the boundary conditions.

To provide examples on how harvested rainwater can be used for the irrigation of VGS within the urban context, two RWH scenarios were developed. The RWH scenarios show how a RWH system can be installed best in different urban areas. For the RWH scenarios, two contrary urban density scenarios were chosen (Figure 5). The two scenarios are distinguished by two variables, namely the degree of development and the building density. The degree of development is the ratio of building area to gross ground area, while the building density is the ratio of the floor area to the ground area (Simperler *et al.*, 2018). Scenario A shows how RWH can be implemented in an urban area with a low degree of development and building density. Scenario B describes the RWH in an urban area with a high degree of development and building density. For both scenarios, an optimal RWH system was described, including the surfaces contributing to run-off, the resulting treatment requirements and the location of the system. To analyse the suitability of roof and street surface run-off for each scenario, the scenario's characteristics regarding housing structure, surface availability, surface pollution, and ownership structure were identified. Further literature research was carried out to identify the required treatment facilities. The possible locations of the RWH system were chosen to be either on a single building scale or a block scale, based on the paper of Angrill *et al.* (2012).





Figure 5: Areal view of urban structure with a) low degree of development and building density, and b) high degree of development and building density (Simperler *et al.*, 2018).

## 4.2 VGS database

The data for the database was gathered from experimental sites at TU Berlin, from VGS installed by the Institute of Soil Bioengineering and Landscape Construction at the University of Natural Resources and Life Sciences, Vienna, and from literature.

A total of 18 VGS have been collected in the database. Information gathered included general details about the system, the location, the system design, the planting and the water supply. To compare the water demand data of the different sites, the information was standardized where possible.

### 4.2.1 Calculation method

For comparability, the water demand and irrigation amounts were converted to  $\text{m}^3 \cdot \text{year}^{-1}$  and  $\text{L} \cdot \text{day}^{-1}$ . If reasonable, averages of the values and the standard deviation was calculated.

For the sites Kandl\_Techmetal, Kandl\_Optigrün, Schuhmeier\_Techmetal and Diefenbach\_Optigrün monthly values of water meter measurements were given (Zluwa, 2019).

Some of the greeneries have irrigation systems controlled by soil moisture sensors. This is the case for site MA31 (Technische Universität Wien and Universität für Bodenkultur Wien, 2018), Mexico\_VGS (Sánchez-Reséndiz *et al.*, 2018) and StAnna (Zluwa, 2019).

The lysimeter measurements were conducted for SiteC\_Berlin and the original data was given as daily averages in  $\text{g} \cdot \text{min}^{-1}$ . To receive monthly sap flow values for each strand, the half-hourly values of the whole month were averaged. These monthly averages are converted in  $\text{L} \cdot \text{day}^{-1}$ , assuming a water density of  $1 \text{ g} \cdot \text{cm}^{-3}$  (Hoelscher, 2018). According to Hoelscher (2018) the evaporation rate can be regarded as negligible.

Sap flow data is given for SiteA\_Berlin and SiteB\_Berlin. For each site, the sap flow measurement devices were placed on several plant strands ("Pflanzenstrang"). Half-hourly sap flow values were given for each strand in  $\text{kg} \cdot \text{h}^{-1}$ . The monthly average was calculated based on these daily averages, converting them in  $\text{L} \cdot \text{day}^{-1}$  as done for the lysimeter measurements above. As these two sites are green facades, it can be concluded that evaporation can also be neglected as done for the lysimeter measurements of SiteC\_Berlin above.

The course of ET throughout the year was given for the sites Madrid\_VGS, Planter box\_Eindhoven and Panel\_Eindhoven. In all three studies, ET was determined from the water balance. The variables were measured separately to conclude about ET rates. Combined with



ET<sub>0</sub>, the development of ET was calculated with the WUCOLS method for Madrid\_VGS (Segovia-Cardozo *et al.*, 2019) and the PM equation for Planter box\_Eindhoven and Panel\_Eindhoven (Van de Wouw *et al.*, 2017).

The course of water demand throughout the year was given for the site Melbourne\_VGS in L.m<sup>-2</sup>.month<sup>-1</sup>, based on water balance measurements (Prodanovic *et al.*, 2019).

### 4.2.2 Location

Information collected about the location of the VGS are the climate zone and the aspect of the VGS. The climate zones were assigned according to the Updated world map of the Köppen-Geiger climate classification by Peel *et al.* (2007).

### 4.2.3 System design

Data collected about the system design are VGS type, geometry, greened area, total substrate volume, substrate composition and hydraulic soil parameters. For the analysis, the variables VGS type, greened area, biomass and substrate volume were chosen. The VGS type was distinguished between green facades as well as between modular and continuous living walls as explained in Chapter 3.1.

The greened area (m<sup>2</sup>) was chosen as the vertical area of the VGS. An exception is the site MA31, for which the greened area does not only include the vertical trellises (with an assumed coverage of 2/3rd), but also the horizontal planted area.

The water demand related to the greened area (L.m<sup>-2</sup>.day<sup>-1</sup> and m<sup>3</sup>.m<sup>-2</sup>.year<sup>-1</sup>) was calculated by dividing water amount by the total greened area in m<sup>2</sup>. Due to a lack of information, the greened area had to be kept constant throughout the vegetation period for all sites, except SiteC\_Berlin (course of greened area derived from pictures taken throughout the measurement period). The water demand related to the greened area for the sap flow measurement of SiteA\_Berlin and SiteB\_Berlin had to be calculated differently. As the measurement devices were attached to single strands, the water demand had to be related to the wall area (WA) of each strand. For each strand, the leaf area (LA) in m<sup>2</sup> and the wall leaf area (WLAI) index was given. The WLAI is the quotient of the LA and the WA. This relation was used to calculate the WA and the water demand per greened area of each strand. The water demand per greened area for the whole VGS was calculated as the average of the values for each strand.

The relative substrate volume (m<sup>3</sup>.m<sup>-2</sup>) was calculated as the total substrate per greened area. Since the total substrate volume of SiteA\_Berlin and SiteB\_Berlin are unknown, this parameter was not calculated.

The water demand related to the substrate volume in L.m<sup>-3</sup>.day<sup>-1</sup> was calculated by dividing the total water amount in L.day<sup>-1</sup> by the substrate volume in m<sup>3</sup>.

### 4.2.4 Planting

The planting specifications are considered by collecting information on the plant species used, the total plant number, and on the plant biomass. This information was combined to obtain the relative plant number and the relative biomass of the VGS.

The relative plant number (number.m<sup>-2</sup>) is the number of plants per square meter of greened area. For modular living walls, the plant number is divided by the horizontal area. For continuous living walls, the plant number is divided by the vertical area. As the green facades only consist of one plant, the relative plant number was not calculated for the green facades.

The water demand related to the plant number in L.plant<sup>-1</sup>.day<sup>-1</sup> was calculated by dividing the total water amount in L.day<sup>-1</sup> by the plant number.

The relative biomass (g.m<sup>-2</sup>) is the biomass of the VGS per square meter of greened area. Data for biomass calculation was only given for the sites Kandl\_Techmetal, Schuhmeier\_Techmetal, Kandl\_Optigrün and Diefenbach\_Optigrün. The average dry mass of the plant species used in

the VGS was calculated based on the values from Scharf and Pitha (2014). This average value was multiplied with the plant number to receive the total biomass in grams. This total biomass was divided by the greened area to receive the relative biomass. For MA31, a different approach was used. The biomass was calculated separately for climbing plants (data source: Pelko (2018)) and perennials (data source: Technische Universität Wien and Universität für Bodenkultur Wien (2018)). To receive the total biomass, the two values were summed up.

The water demand related to the biomass in  $\text{L.g}^{-1}.\text{day}^{-1}$  was calculated by dividing the total water amount in  $\text{L.day}^{-1}$  by the total biomass in g.

## 5. Results and discussion

### 5.1 Conceptual model

The conceptual model is shown in Figure 6. It illustrates the processes influencing the irrigation demand of VGS and how RWH can contribute to supply the water needed. The main parts of the model – the VGS and the RWH – are described in this chapter.

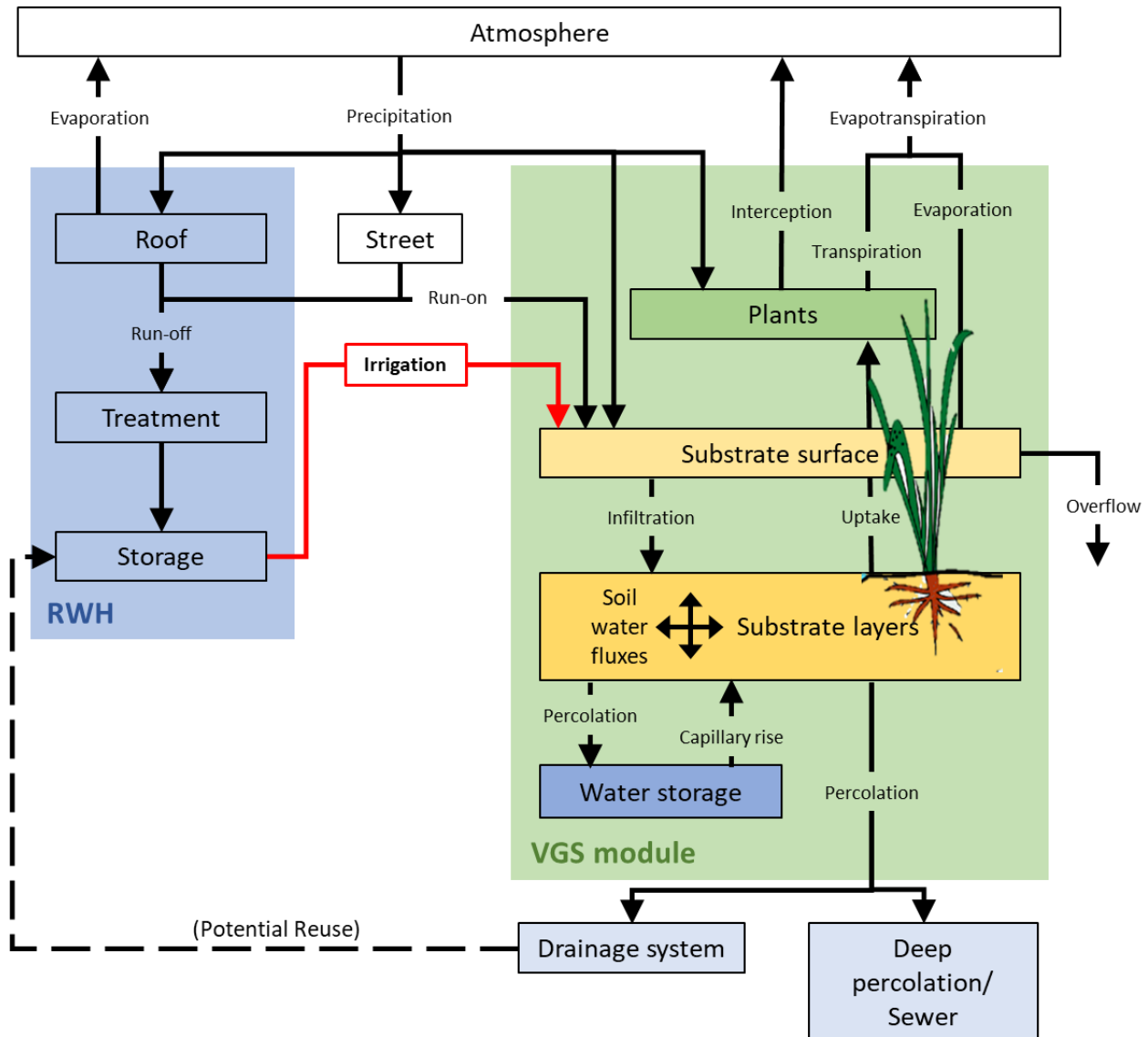


Figure 6: Conceptual model.

The VGS part (green box) is based on the water balance and the features of VGS described in Chapter 3.1. During a precipitation event, precipitation falls directly on the substrate and flows onto the substrate from surrounding areas. Precipitation falling on the vegetation surfaces is lost as interception. From the substrate surface, the water partly infiltrates into the substrate layers and is partly lost by evaporation. In the substrate layers, the soil water fluxes are driven by gravity and soil water potential gradients. If the water in the substrate layer exceeds FC, it cannot be held against gravity and the water percolates either into the water storage, into deeper soil layers or drains out of the system. The water storage is created through an impoundment, which is filled until the design allows (impoundment depth) and is emptied due to capillary rise driven by the soil water potential gradient. Percolation water can either be captured in a drainage system for water

recirculation to the RWH storage tank. If no drainage system is installed, water is lost either through deep percolation or discharge to the sewer system.

Looking at the RWH part (blue box), precipitation reaches impermeable surfaces such as roofs and streets from where it contributes to run-off. The run-off amount is influenced by “climatic (size and intensity of the rain event, antecedent moisture, prevailing winds) and architectural (slope, roof material, surface depressions, leaks/infiltration, roughness)” (Singh et al., 2013) factors. Run-off is generated and directed to the treatment system. From there, it is further directed to a storage tank. If it is foreseen in the system, drainage water from the VGS can be additionally collected in the storage tank.

Similar conceptualisations of hydrological processes have been successfully applied to green stormwater facilities (Herrera *et al.*, 2017), “blue-green” infrastructure (Rozos *et al.*, 2013) and green roof modelling (Mobilia *et al.*, 2017). The RWH part of the conceptual model can be compared to the visualisation of RWH in the urban environment by Angrill *et al.* (2012). Stratigea and Makropoulos (2015) developed a model to combine RWH, greywater reuse and green roof run-off as stormwater infrastructure.

### 5.1.1 Governing equations

In this chapter, the governing equations for the assessment of the VGS water demand and the storage sizing of the RWH system are presented. The assessment of the VGS water demand is based on the water balance. Depending on the time step chosen, this can lead to major inaccuracies of the estimated water demand. Assuming a time step of one day, the diurnal variations of the water demand (e.g. during day and night) will not be reflected in the results. Furthermore, the VGS type (see Chapter 3.1) influences the water demand calculation as the water in- and outputs are changing. The resulting boundary conditions for each type are described in more detail in Chapter 5.1.3.

The equations of the VGS concentrate on supplying the plants with water to ensure a good plant development. For optimal plant growth, the water volume in the substrate needs to be easily extractable by the plant. Theoretically, the plants can take up water when the water content is between FC and PWP. Practically, the plant water uptake is already reduced before the water content at the PWP is reached. This threshold soil water volume is defined as the readily available water (RAW) (Allen *et al.*, 1998),

$$V_{RAW} = p \times (\theta_{FC} - \theta_{PWP}) \times V_s \quad (5)$$

where:

$V_{RAW}$  is the readily available water volume (L<sup>3</sup>);

$p$  is the average fraction which can be depleted before moisture stress (-);

$\theta_{FC}$  is the water content at field capacity (-);

$\theta_{PWP}$  is the water content at the permanent wilting point (-); and

$V_s$  is the substrate volume (L<sup>3</sup>).

Depending on the ET rate,  $p$  ranges from 0.3 to 0.7. For many crops, a value of 0.5 is assumed (Allen *et al.*, 1998).

The water volume at time  $t$  in a VGS module is generally described as:

$$V_{m,t} = V_{m,t-1} + \Delta t \times (In_{m,t} - Out_{m,t}) \quad (6)$$

where:

$t$  is the time index (T);

$m$  is the module index (-);

$V$  is the water volume in the substrate ( $L^3$ );

$In$  is the total water input ( $L^3.T^{-1}$ ); and

$Out$  is the total water output ( $L^3.T^{-1}$ ).

The optimal irrigation must ensure a healthy plant growth, while reducing percolation losses. Hence, the water content in the substrate should be between the RAW and the FC. If the water volume in the substrate drops below  $V_{RAW}$ , additional water input is needed. The irrigation amount should fill the soil water storage until FC is reached. The total irrigation amount is:

$$\begin{cases} V_{m,t} > V_{RAW} \rightarrow I_t = 0 \\ V_{m,t} \leq V_{RAW} \rightarrow I_t = \sum_{m=1}^n \frac{V_{FC} - V_{m,t}}{\Delta t} \end{cases} \quad (7)$$

with

$$V_{FC} = \theta_{FC} \times V_s \quad (8)$$

where:

$I$  is the irrigation amount ( $L^3.T^{-1}$ );

$n$  is the total number of modules (-); and

$V_{FC}$  is the water volume at field capacity ( $L^3$ );

Including all flow paths, the water in- and outputs to one VGS module can be described as:

$$In_{m,t} = P_{m,t} + Q_{run-on\ m,t} + Q_{overflow\ m-1,t} + Q_{p\ m-1,t} \quad (9)$$

$$Out_{m,t} = ET_{m,t} + Q_{p\ m,t} + Q_{overflow\ m,t} \quad (10)$$

where:

$P$  is the precipitation reaching the substrate surface ( $L^3.T^{-1}$ );

$Q_{run-on}$  is the run-on volume from surrounding areas ( $L^3.T^{-1}$ );

$Q_{overflow}$  is the overflow volume from the module above ( $L^3.T^{-1}$ );

$ET$  is the evapotranspiration ( $L.T^{-1}$ ); and

$Q_p$  is the percolation ( $L^3.T^{-1}$ ).

Precipitation reaching the substrate for infiltration was estimated as the share of precipitation collected (see Van de Wouw *et al.* (2017)) minus the water lost from the vegetation surface by evaporation (formula based on Herrera *et al.* (2017)):

$$P_t = h_t \times A_s \times r - \frac{E_s}{\Delta t} \times A_g \quad (11)$$

with

$$E_s = LAI \times ET_0 \times t_s \quad (12)$$

where:

$A_s$  is the substrate area ( $L^2$ );

$r$  is the reduction coefficient as defined by Van de Wouw *et al.* (2017) (-);

$E_s$  is the water lost as evaporation ( $L$ );

$A_g$  is the greened area ( $L^2$ );

$LAI$  is the leaf area index (-); and

$t_s$  is the time from the beginning of the storm (T).

The run-on can be calculated according to a simplified rational method (compare ÖNORM EN 16941-1 (2018)) as:

$$Q_{run-on} = A \times RC \times h_t \quad (13)$$

where:

$A$  is the horizontal projection of the area contributing to run-on ( $L^2$ );

$h$  is the precipitation height ( $L.T^{-1}$ ); and

$RC$  is the surface yield coefficient or run-off coefficient (-).

Following the example of green roof run-off estimation by Rozos *et al.* (2013), the overflow can be calculated as:

$$\begin{cases} V_t \leq V_{max} \rightarrow Q_{overflow} = 0 \\ V_t > V_{max} \rightarrow Q_{overflow} = \frac{V_t - V_{max}}{\Delta t} \end{cases} \quad (14)$$

where:

$V_{max}$  is the maximum water volume that can be retained in the VGS ( $L^3$ ).

For ET calculation, the antecedent precipitation index (API) model was chosen, as it already has been used successfully by Mobilia *et al.* (2017) for green roof modelling and no calibration is needed. The actual ET is calculated as a share of the potential ET based on the formula of Priestley-Taylor (Priestley and Taylor, 1972):

$$AET = 0.408\alpha \left[ \frac{\Delta}{\Delta + \gamma} (R_n - G) \right] \quad (15)$$

where:

$AET$  is the actual evapotranspiration flux ( $M.L^{-2}.T^{-1}$ );

$\alpha$  is the reduction coefficient (-);

$\Delta$  is the slope of the saturation vapour pressure-temperature curve ( $M.L^{-1}.T^{-1}.\theta^{-1}$ );

$R_n$  is the net radiation ( $M.T^{-3}$ );

$G$  is the soil heat-flux density at the soil surface ( $M.T^{-3}$ ); and

$\gamma$  is the psychrometric constant ( $M.L^{-1}.T^{-1}.\theta^{-1}$ ).

The slope of the saturation vapour pressure-temperature is calculated as:

$$\Delta = \frac{4098 \left[ 0.6108 \exp \left( \frac{17.27 T_{mean}}{T_{mean} + 237.3} \right) \right]}{(237.3 + T_{mean})^2} \quad (16)$$

where:

$T_{mean}$  is the average temperature between maximum and minimum values ( $\theta$ ).

The coefficient  $\alpha$  is calculated as:

$$\begin{cases} \text{if } API \leq 20 \text{ mm} \rightarrow \alpha = 0.123(API) - 0.0029(API)^2 - 0.0000056(API)^3 \\ \text{if } API > 20 \text{ mm} \rightarrow \alpha = 1.26 \end{cases} \quad (17)$$

where:

$API$  is the antecedent precipitation index (L).

The  $API$  for each day is the sum of the weighted daily precipitation depths for the last 28 days (Marasco, 2014)

$$API_d = \sum_{t=1}^{28} K^{t-1} \times P_{d-t} \quad (18)$$

where:

$d$  is the index for the day (T);

$t$  is the index for the previous days (T); and

$K$  is the dimensionless recession constant, set to 0.9 (-).

To use the total ET per time step in Equation (10), the actual ET must be converted as:

$$ET = \frac{AET}{\rho_w} \times A_g \quad (19)$$

where:

$\rho_w$  is the water density (M.L<sup>-3</sup>).

As used in Herrera *et al.* (2017) for green stormwater facilities, the percolation discharge from one module can be calculated with the percolation rate (Savabi and Williams, 1995) as

$$\begin{cases} V_t \leq V_{FC} \rightarrow Q_p = 0 \\ V_t > V_{FC} \rightarrow Q_p = A_d \times p_e = A_d \times \left( (\theta_t - \theta_{FC}) \left( 1 - e^{-\frac{\Delta t}{t_t}} \right) \frac{d}{\Delta t} \right) \end{cases} \quad (20)$$

where:

$p_e$  is the percolation rate (L.T<sup>-1</sup>);

$A_d$  is the area of the drainage opening (L<sup>2</sup>);

$\theta_t$  is the water content in this time step (-);

$t_t$  is the travel time through the module/layer (T); and

$d$  is the thickness of the module/layer (L).

The travel time  $t$  can be written as

$$t_t = \frac{\theta_t - \theta_{FC}}{k_{unsat}} d \quad (21)$$

where:

$k_{unsat}$  is the unsaturated hydraulic conductivity in the module/layer (L.T<sup>-1</sup>).

The unsaturated hydraulic conductivity can be calculated according to the formula used by Herrera *et al.* (2017).

The sizing of the RWH storage tank is based on mass balance equations of the inflows and outflows, which are calculated with the rainwater yield and the water demand, respectively.

The rainwater yield after treatment can be calculated according to Equation (22) as a share of the total precipitation falling on the surface. This formula is based on the rational method as found in Dingman (2015), which has been simplified for an easier application (ÖNORM EN 16941-1, 2018)

$$Y_{r,t} = A \times h_t \times RC \times \eta \quad (22)$$

where:

$Y_r$  is the rainwater yield ( $L^3.T^{-1}$ ); and

$\eta$  is the hydraulic treatment efficiency coefficient specified by the manufacturer (-).

The optimal storage size should be calculated with an input-output simulation to take into account the irregular water demand, which is the case for the irrigation demand of VGS (see changes of ET rates throughout the day and the season, as shown in Allen *et al.* (1998)). ÖNORM EN 16941-1 (2018) proposes the following approach:

$$S_{r,t} = \min \left\{ I_t, V_{r,(t-1)} \right\} \quad (23)$$

$$\begin{cases} V_{r,(t-1)} < V \rightarrow V_{r,t} = V_{r,(t-1)} + Y_{r,t} - S_{r,t} \\ V_{r,(t-1)} = V \rightarrow V_{r,t} = V - S_{r,t} \end{cases} \quad (24)$$

where:

$S_r$  is the abstraction from the tank ( $L^3.T^{-1}$ );

$V_r$  is the rainwater volume in the storage tank ( $L^3$ ); and

$V$  is the useable volume of the tank ( $L^3$ ).

To find the optimal tank size, the coverage rate is calculated for a range of storage volumes:

$$C_r(V) = \frac{\sum_t S_{r,t}}{\sum_t I_t} \quad (25)$$

where:

$C_r(V)$  is the coverage rate for a selected storage volume (-).

The coverage rate is plotted against the storage volume. The resulting curve helps to determine the optimal storage volume, which should ideally cover 100% of the water demand of the VGS. If this is not achievable with only rainwater, alternative sustainable water sources such as greywater should be considered (Sánchez-Reséndiz *et al.*, 2018).

### 5.1.2 Discussion of conceptual model

In this chapter, the choice of equations for the calculation of the VGS water demand are discussed.

The reduction coefficient  $r$  used for the calculation of the collected precipitation (Equation (11)) determines the share of precipitation, which can be collected in a VGS. Based on a mass balance approach, Van de Wouw *et al.* (2017) derived the following values for an individual event: 18.8% for a continuous living wall and 33% for a modular living wall (Van de Wouw *et al.*, 2017). These values must be handled with care as they have only been calculated for a specific type of VGS and for a specific location. If the water balance components (precipitation, irrigation, ET, through flow, and run-off) are measured, the reduction coefficient can be calculated as the relation between collected precipitation (mass gain of the system) to the precipitation fallen on a horizontal



square meter (compare Van de Wouw *et al.* (2017)). To gather more knowledge about how precipitation is collected in VGS, this method should be applied to the three different types of VGS in several locations.

The overflow estimation (Equation (14)) chosen for the model is based on the comparison of the maximum retainable water volume to the actual water volume in the VGS module. The physical and chemical soil characteristics, such as the infiltration rate, the soil constitution or the hydrophobicity of the soil, are neglected for simplification reasons. However, they are certainly influencing the infiltration rate and thereby the resulting overflow rate from the system (Amelung *et al.*, 2018). Still, the level of detail resulting from the volume approach is reasonable for the here presented water demand calculation, as it has already been used successfully for the overflow estimation of green roofs (Rozos *et al.*, 2013).

The equation chosen for the calculation of ET (Equation (15)) is based on the approach by Priestley-Taylor. This equation considers radiation and assumes a “wet vegetated surface with minimal advection” (Marasco, 2014). This might lead to inaccurate results as the effect of advection should only be neglected for “large, extensive surfaces of homogeneous vegetation” (Allen *et al.*, 1998), which is not the case for VGS, hence, advection should be included. An alternative calculation approach is the Penman-Monteith method. The Penman-Monteith method requires more information about the local weather than the Priestley-Taylor approach. This data is used for the calibration (with a crop coefficient  $K_c$ ) to the location of interest. The crop coefficient  $K_c$  is calculated by comparing the measured ET with the  $ET_0$  calculated with the Penman-Monteith equation. This has been done for a green facade (Hoelscher, 2018), a continuous living wall and two modular living walls (Segovia-Cardozo *et al.*, 2019; Van de Wouw *et al.*, 2017). Segovia-Cardozo *et al.* (2019) used the WUCOLS III approach to calculate the landscape coefficient  $K_L$ , which results in  $K$  values for the initial phase, mid-season and end-season. Table 1 shows the derived  $K_c$  values. The coefficients of determination show that even for a single location, the obtained linear regressions (between the measured and the reference ET) describe a range of 28 to 94% of the data. Feng (2019) mentions the difficulty of reusing microscale-calibrated models for other locations. Whether the use of these  $K_c$  values for other locations can deliver precise results has to be investigated in future research. Comparing the two methods, the Priestley-Taylor method might deliver less accurate results due to the neglect of advection. However, the choice of the method is still reasonable for the calculation of the water demand, because no calibration is needed as would be for the Penman-Monteith equation.

Table 1: VGS  $K_c$  values from literature for Penman-Monteith modelling of ET.

VGS type	Value	Coefficient of determination
Green facade <i>Fallopia baldschuanica</i> <sup>[1]</sup>	$K_c = 1.25$	$R^2 = 0.51$
Modular living wall <sup>[2]</sup>	$K_c = 0.76$	$R^2 = 0.28$
Modular living wall (WUCOLS III method) <sup>[3]</sup>	$K_{L\text{ ini}} = 0.32$ $K_{L\text{ mid}} = 0.60$ $K_{L\text{ end}} = 0.38$	$R^2 = 0.94$
Continuous living wall <sup>[2]</sup>	$K_c = 1.46$	$R^2 = 0.70$

<sup>[1]</sup> Hoelscher (2018), <sup>[2]</sup> Van de Wouw *et al.* (2017), <sup>[3]</sup> Segovia-Cardozo *et al.* (2019).

The calculation of the run-off yield for RWH (Equation (22)) requires the determination of a run-off coefficient (RC). Average RC values are ranging from 0.70 to 0.95 for urban environments (Farreny *et al.*, 2011). To receive a precise RC value for the site investigated, the RC should be determined by experimental studies or hydrological models. Examples from literature for the determination are Farreny *et al.* (2011) in Spain and Romaniak (2017) in Poland.

Furthermore, alternative approaches for run-off modelling have been investigated by several research groups. Singh *et al.* (2013) compared popular hydrological models (SCS-CN and some of its variants) to the Central Ground Water Board method (similar to Equation (22)) and the roof run-off from a single building generated with the different approaches. Walsh *et al.* (2014) analysed the watershed reductions due to RWH using U.S. Environmental Protection Agency's

Storm Water Management Model (SWMM). Due to the focus on the watershed-scale, the demand patterns of the households were neglected. Green roof run-off modelling has been conducted by Herrera *et al.* (2018) using the IHMORS hydrological model in Chile and Mobilia *et al.* (2017) using a water balance conceptual model in Germany.

In the course of this thesis, the model could not be validated so further research is needed to see how the model performs. Especially the influence of the microclimatic fluctuations on the water demand of VGS should be investigated in more detail. Hopkins and Goodwin (2011) mention temperature and humidity, wind, and orientation to be especially influential. They recommend collecting daily data of local temperature and humidity to be able to reveal and consider extremes. Taha (1997) indicates that the urban temperature is also increased due to human activities including for example cars and air-conditioning. To what extent these local temperature differences influence the water demand of VGS has to be investigated in more detail. Regarding precipitation data, daily values should be used to avoid the averaging of long drought periods by single storm weather events. Furthermore, wind turbulences at corners and edges stress the system and plants. Wind speed and direction thereby influence the substrate humidity (Hopkins and Goodwin, 2011) and subsequently their water demand. Also, the orientation of the VGS has an impact on how much stress the plants are exposed to. Shadows cast by surrounding buildings can reduce day-light and reflections from opposite buildings can increase radiation (Hoelscher, 2018; Riley, 2017). These changes in radiation can lead to locally induced differences in water demand.

### 5.1.3 VGS boundary conditions

The boundary conditions describe the differences in the water demand calculation for the two main VGS types: Living walls and green facades. Due to the system design, the in- and output parameters for Equation (9) and (10) vary for the two types. The resulting in- and output equations are presented in this chapter.

Modular and continuous living walls receive water input from precipitation  $P$  reaching the substrate surface and overflow from saturated modules above, but do not receive water as run-on from surrounding areas. The outputs are ET, percolation discharge  $Q_p$  and the overflow  $Q_{overflow}$ . These components are influential factors on the water balance of a living wall module (Van de Wouw *et al.*, 2017). The overflow from these systems is dependent on the maximum water volume  $V_{max}$  retainable in the VGS (see Equation (14)). For modular living walls,  $V_{max}$  is dependent on the maximum freeboard. For continuous living walls on the other hand,  $V_{max}$  is equal to the water volume in saturated condition.

The in- and output formulas for one module of these systems is therefore as follows:

$$In_{living\ wall\ m} = P_m + Q_{overflow\ m-1} + Q_{p\ m-1} \quad (26)$$

$$Out_{living\ wall\ m} = ET_m + Q_{p\ m} + Q_{overflow\ m} \quad (27)$$

For green facades a distinction must be made between green facades planted in a pot and those planted in soil. The total water input includes precipitation falling on the substrate and, if the facade is planted in the soil, the run-on from surrounding areas. Green facades do not consist of several modules (total number of modules  $n = 1$ ), therefore they do not receive overflow from other modules. The output is ET,  $Q_p$  and  $Q_{overflow}$ . If the green facade is planted in a pot, Equations (26) and (27) apply. If it is planted in the soil, its construction can be compared to a bio-retention cell as found in the SWMM Reference Manual by Rossman and Huber (2016). The overflow discharge  $Q_{overflow}$  (see Equation (14)) is again dependent on the system design and whether the green facade is planted in a pot or in the soil. If the green facade is planted in a pot,  $V_{max}$  is dependent on the maximum freeboard, if the green facade is planted in the soil,  $V_{max}$  is equal to the water volume in saturated condition. Compared to Rossman and Huber (2016), ET is not split into ET from different substrate layers, but is assumed to be one total value for the whole system.

The percolation discharge  $Q_p$  is lost to the underlying ground and  $A_d$  in Equation (20) has to be equal to the total ground area of the facade.

The in- and output formulas for green facades are written as:

$$In_{green\ facade} = P + Q_{run-on} \quad (28)$$

$$Out_{green\ facade} = ET + Q_p + Q_{overflow} \quad (29)$$

### 5.1.4 RWH scenarios

The equations for the dimensioning of the RWH systems will not change depending on the scenario chosen. However, the size of the surface area contributing to run-off, the corresponding RC and the hydraulic treatment efficiency (Equations (22) to (25)) will change.

Scenario A describes the RWH in urban areas with a low building density and a low degree of development. This urban structure type is characterised by detached houses with one to two floors, a high surface availability, a low surface pollution, and a heterogeneous ownership structure (Simperler *et al.*, 2018).

In this scenario, VGS will be installed on single-family houses. To avoid long RWH network connections, the suggested RWH location for scenario A is at the building-scale. Furthermore, the heterogeneous ownership structure (many different owners of single buildings) results in a high need for coordination, which reduces the implementation potential of centralized measures (Simperler *et al.*, 2018). This is supported by the life cycle assessment of Angrill *et al.* (2012), who suggest a RWH system at building scale for low density areas as in scenario A. The recommended storage types are a RWH tank distributed over the roof or an underground tank (Angrill *et al.*, 2012).

The low degree of development in scenario A results in a high surface availability but a low share of sealed surfaces (Simperler *et al.*, 2018). Generally, the areas available for rainwater run-off collection are rooftop and street areas. The treatment requirements for run-off collection from these two surfaces are different. For collected roof run-off, mechanical filtration and sedimentation are sufficient. However, the collection of street run-off requires more elaborate treatment (Matzinger *et al.*, 2017). If the demand can be covered with collected rainwater from roof areas, this should be the first choice for scenario A. The lower treatment requirements of roof run-off result in a higher economic efficiency for single building owners. This might be the reason why literature research on the use of street surface run-off for rainwater collection in low density areas does not deliver any results to the author's knowledge. Street run-off is most often handled in stormwater management plans with the goal of reducing the amount of run-off diverted to the sewer system. Nevertheless, the collection of street run-off can be considered in case of high demand for service water.

Scenario B describes RWH in urban areas with a high building density and high degree of development. This urban structure type is characterised by a closed building structure, which is typical for city centres. This scenario has a low surface availability, a high surface pollution and a more homogenous ownership structure than scenario A (Simperler *et al.*, 2018).

The high degree of development results in a higher share of sealed surfaces, which is a good prerequisite for RWH. Generally, more water is consumed in dense areas (Nolde, 2007). To cover the demand of non-potable water with harvested rainwater, more run-off needs to be captured. Therefore, it should be considered to not only use roof run-off, but also run-off from more polluted surfaces such as roads. As mentioned above, the higher pollution of street run-off requires a higher treatment effort (Nolde, 2007). Sojka *et al.* (2016) state that street runoff is not a feasible source due to its pollution level. Pet waste, motor oil, de-icing salts etc. significantly increase the treatment requirements compared to roof run-off. However, this statement is questioned by the findings of Nolde (2007) who investigated a treatment system for run-off from roofs, courtyards, sidewalks and traffic surfaces with a low traffic density. In this study, the characteristics of the

traffic surfaces (such as the annual average daily traffic) are not mentioned. Still, this is a key information for assessing the suitability of traffic surfaces for RWH. In Austria, the run-off from surface areas is classified according to ÖWAV-Regelblatt 45 (2015). Future research is needed to investigate the changes in treatment requirements for RWH from street surfaces with different traffic loads. Additional research on the financial benefits of RWH from street surfaces would be of great interest.

On a building scale, Nolde (2007) presented a possible treatment system for run-off from roofs, courtyards, sidewalks and traffic surfaces with a low traffic density. The treatment includes a sediment grit chamber, a biological treatment with a planted substrate filter and UV disinfection, located in the basement of an apartment building. The effluent of the treatment system has a good water quality, even exceeding the water quality requirements of the EU Directive for Bathing Water (Nolde, 2007). This contradicts the statement by Sojka *et al.* (2016) that ground-level surfaces are not the preferred source for RWH because of their pollution level.

On a block scale, a central collection tank can be located either in the courtyard or in the basement of one building. Depending on the water demand quantity, the surrounding roof and/or street areas act as catchment surfaces. Due to the more homogenous ownership structure, the installation of a block tank is more realistic than in scenario A. These options are supported by the work of Angrill *et al.* (2012), who found the tank distributed over the roof of a single building and the block tank to be the best options for the “compact density scenario”.





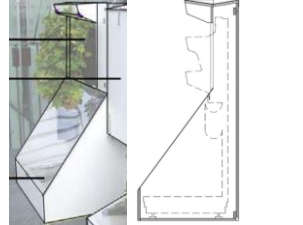



## 5.2 VGS database

In this chapter, the data gathered in the database is presented and analysed. The detailed tables of the database and the results of the water demand and irrigation amount calculation are attached in Appendix 9.1 and 9.2, respectively.


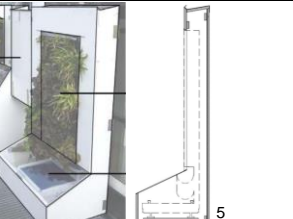
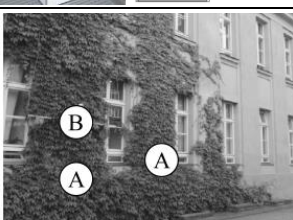
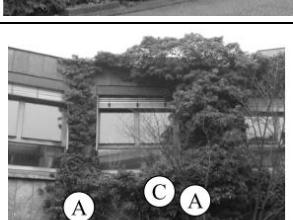

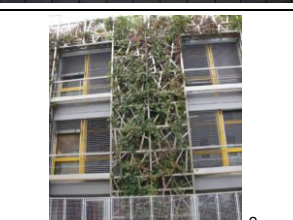
### 5.2.1 Analysis of water demand and irrigation amounts

Not all data related to the irrigation or water demand was comparable to each other. Therefore, a distinction was made between “irrigation amounts” and “water demand”. “Irrigation amounts” are derived from maintenance data, such as water meter measurements. “Water demand” is the actual demand of the plants and the system, which was derived from sap flow and lysimeter measurements, soil moisture-controlled irrigation and ET calculations. Table 2 shows which information was available for each site. Additionally, some general information about the systems is shown.

Table 2: Analysed VGS, type and data available for irrigation demand analysis.

	ID	Address	VGS type	Plant types	Data available	Photo
1	Kandl_ Techmetal	Vienna, Austria	Modular living wall	Perennials	<b>Irrigation amount</b> from water table of water meter	
2	Schuhmeier_ Techmetal	Vienna, Austria	Modular living wall	Perennials	<b>Irrigation amount</b> from water table of water meter	
3	MA31	Vienna, Austria	Modular living wall	Perennials Climbing plants	<b>Water demand</b> from monthly irrigation sums based on water content sensor	
4	Madrid_VGS	Madrid, Spain	Modular living wall	Grasses Fern Perennials	<b>Water demand</b> from ET rates throughout the year based on water balance	
5	Planter box_ Eindhoven	Eindhoven, Netherlands	Modular living wall	No information	<b>Water demand</b> from ET rates throughout the year based on water balance	
6 - 10	Melbourne_ VGS	Melbourne, Australia	Modular living wall	5 different plant types: Grasses Fern Perennials	<b>Water demand</b> from water balance for each plant type	
11	Kandl_ Optigrün	Vienna, Austria	Continuous living wall	Perennials	<b>Irrigation amount</b> from water table of water meter	
12	Diefenbach_ Optigrün	Vienna, Austria	Continuous living wall	Perennials	<b>Irrigation amount</b> from water table of water meter	

## Results and discussion

	ID	Address	VGS type	Plant types	Data available	Photo
13	Mexico_VGS	Querétaro, Mexico	Continuous living wall	Perennials Grasses Climbing plants	<b>Water demand</b> from irrigation sums controlled by soil humidity sensor	
14	Panel_Eindhoven	Eindhoven, Netherlands	Continuous living wall	No information	<b>Water demand</b> from ET rates throughout the year based on water balance	
15	Site A_Berlin	Berlin, Germany	Direct green facade	Climbing plants	<b>Water demand</b> from sap flow measurement	
16	Site B_Berlin	Berlin, Germany	Direct green facade	Climbing plants	<b>Water demand</b> from sap flow measurement	
17	Site C_Berlin	Berlin, Germany	Indirect green facade	Climbing plants	<b>Water demand</b> from lysimeter measurement	
18	StAnna	Vienna, Austria	Indirect green facade	Climbing plants	<b>Water demand</b> from annual irrigation sums controlled by soil moisture sensor	

<sup>1</sup> GrünPlusSchule (2018), <sup>2</sup> GrüneZukunftSchule (2018), <sup>3</sup> Pelko (2018), <sup>4</sup> Segovia-Cardozo *et al.* (2019), <sup>5</sup> Van de Wouw *et al.* (2017), <sup>6</sup> Prodanovic *et al.* (2019), <sup>7</sup> Sánchez-Reséndiz *et al.* (2018), <sup>8</sup> Hoelscher (2018), <sup>9</sup> Zluwa (2019).

The values of the total annual water demand and irrigation amount of the analysed VGS are presented in Figure 7. The values range from 0.03 to 74.71 m<sup>3</sup>.day<sup>-1</sup>, for the site Melbourne\_VGS *Ophiopogon japonicus* and MA31, respectively. As can be seen, values for the green facades SiteA\_Berlin, SiteB\_Berlin and SiteC\_Berlin are missing. This is because no values for the total annual water demand could be derived from the sap flow and transpiration measures (limited measurement period, see Appendix 9.1).

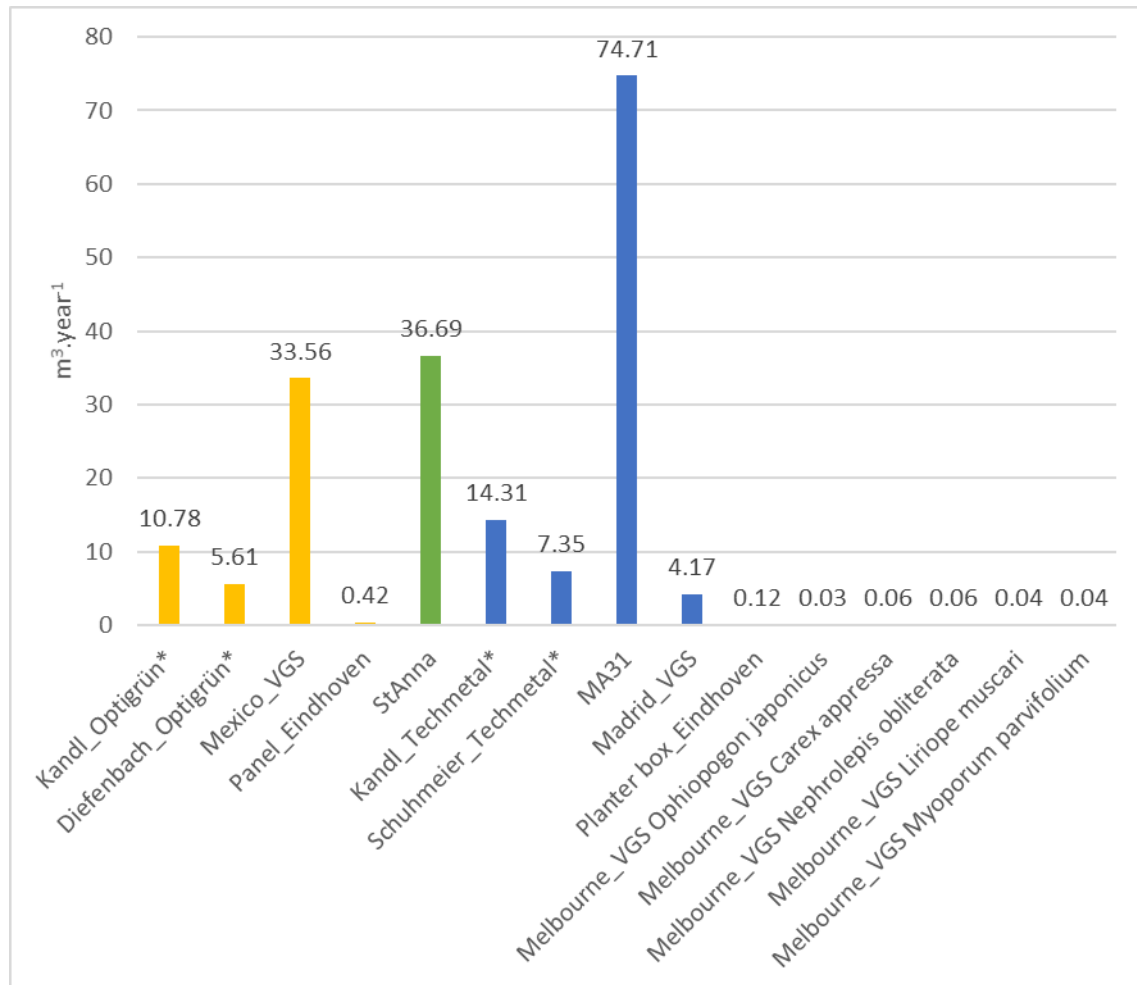


Figure 7: Annual total water demand and irrigation amounts (marked with a star) per m² for continuous living walls (yellow), green facades (green) and modular living walls (blue).

Figure 8 shows the annual water demand and irrigation amounts per square meter of greened vertical area. The maximum value is  $6.15 \text{ m}^3 \cdot \text{m}^{-2} \cdot \text{day}^{-1}$  for the continuous VGS Mexico\_VGS and the minimum value is  $0.28 \text{ m}^3 \cdot \text{m}^{-2} \cdot \text{day}^{-1}$  for the modular VGS Kandl\_Techmetal. Looking at the climatic conditions, the outlier Mexico\_VGS can be explained by being the only VGS located in arid climatic conditions (see Table 3).

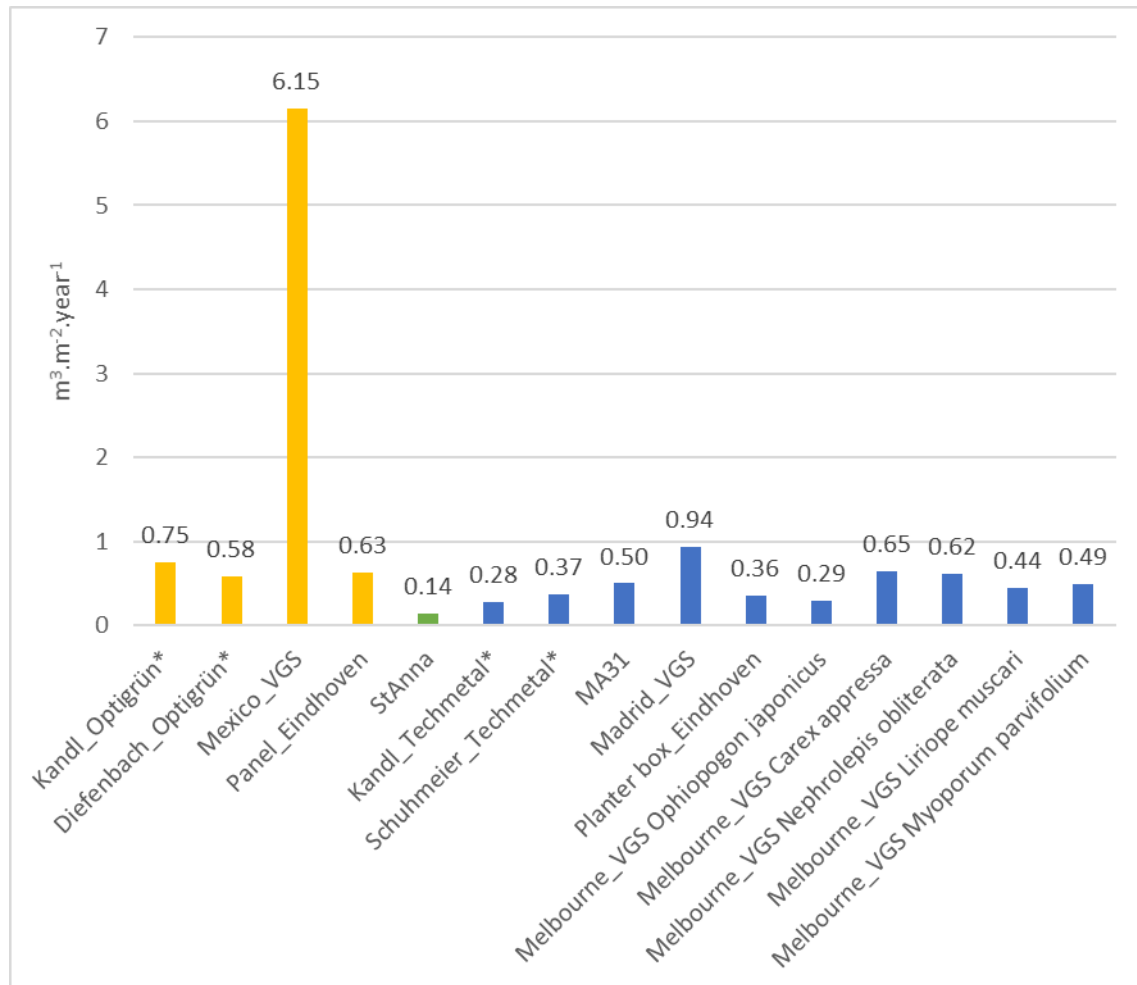


Figure 8: Annual water demand and irrigation amounts (marked with a star) per m² for continuous living walls (yellow), green facades (green) and modular living walls (blue).



Table 3: Köppen-Geiger climate types and general climate classifications after Peel *et al.* (2007). DfB = Warm-summer humid continental climate; Csa = Mediterranean hot summer climate; Cfb = Oceanic climate; BSh = Semi-arid climate.

ID	Location	Climate type	General classification
Kandl_Techmetal	Vienna, Austria	DfB	Cold
Schuhmeier_Techmetal	Vienna, Austria	DfB	Cold
MA31	Vienna, Austria	DfB	Cold
Madrid_VGS	Madrid, Spain	Csa	Temperate
Planter box_Eindhoven	Eindhoven, Netherlands	Cfb	Temperate
Melbourne_VGS	Melbourne, Australia	Cfb	Temperate
Kandl_Optigrün	Vienna, Austria	DfB	Cold
Diefenbach_Optigrün	Vienna, Austria	DfB	Cold
Mexico_VGS	Querétaro, Mexico	BSh	Arid
Panel_Eindhoven	Eindhoven, Netherlands	Cfb	Temperate
Site A_Berlin	Berlin, Germany	DfB	Cold
Site B_Berlin	Berlin, Germany	DfB	Cold
Site C_Berlin	Berlin, Germany	DfB	Cold
StAnna	Vienna, Austria	DfB	Cold

To avoid the bias due to the climatic conditions, Figure 9 shows the annual water demand and irrigation amounts per square meter of greened area without site Mexico\_VGS. The average values and standard deviations for continuous and modular living walls are  $0.65 \pm 0.07$  and  $0.49 \pm 0.19 \text{ m}^3 \cdot \text{m}^{-2} \cdot \text{year}^{-1}$ , respectively. The data for green facades is available for StAnna with an annual water demand of  $0.14 \text{ m}^3 \cdot \text{m}^{-2} \cdot \text{year}^{-1}$ .

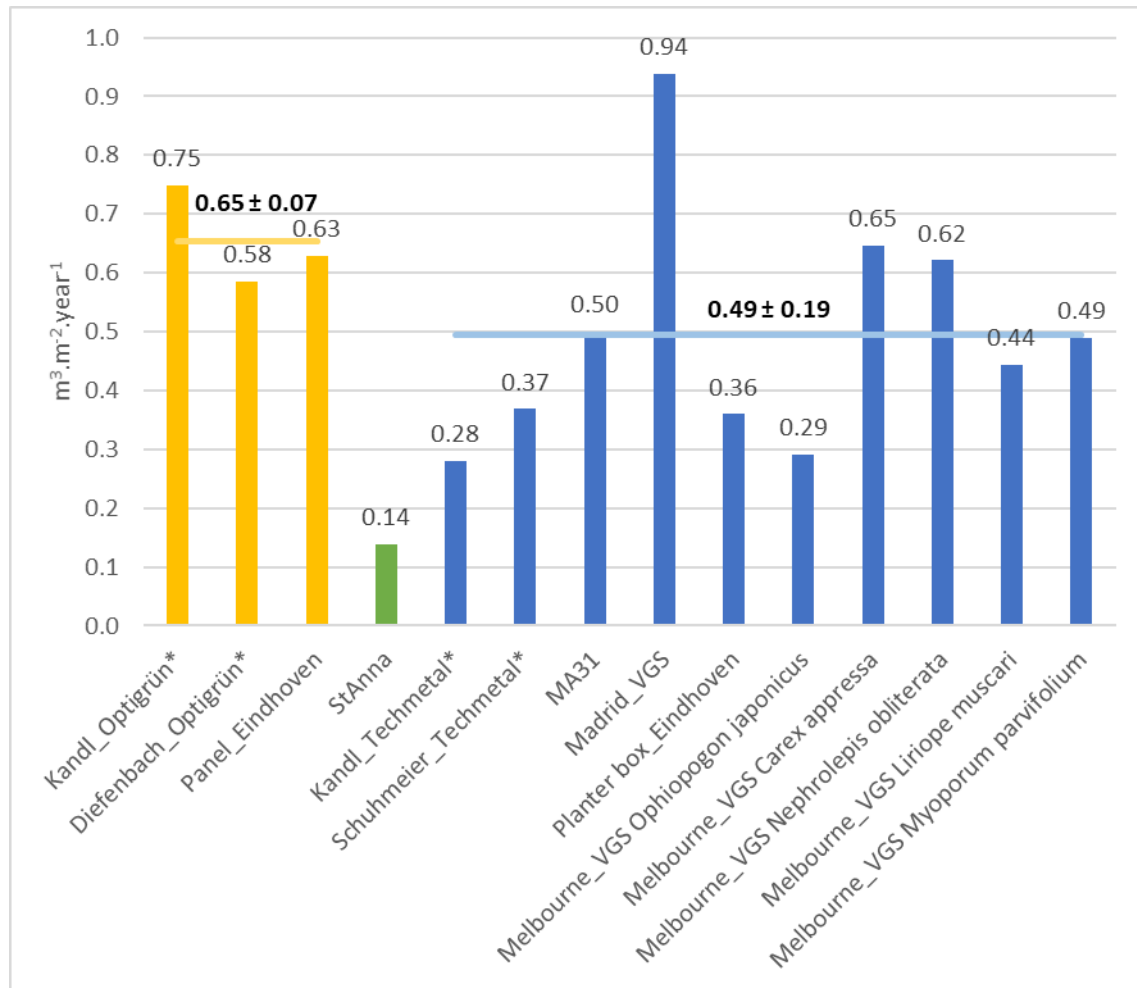


Figure 9: Annual water demand and irrigation amounts (marked with a star) per m<sup>2</sup> for continuous living walls (yellow), green facades (green) and modular living walls (blue). Without Mexico\_VGS.

The daily water demand and irrigation amounts per square meter for a day in summer are shown in Figure 10. For all sites, except the Australian sites, the daily values for August were taken. For the Australian sites, values for February were used due to the different seasons. The averages and standard deviations are  $3.46 \pm 0.85$ ,  $2.40 \pm 1.44$  and  $2.38 \pm 1.34$  L.m<sup>-2</sup>.day<sup>-1</sup> for continuous living walls, green facades and modular living walls, respectively.

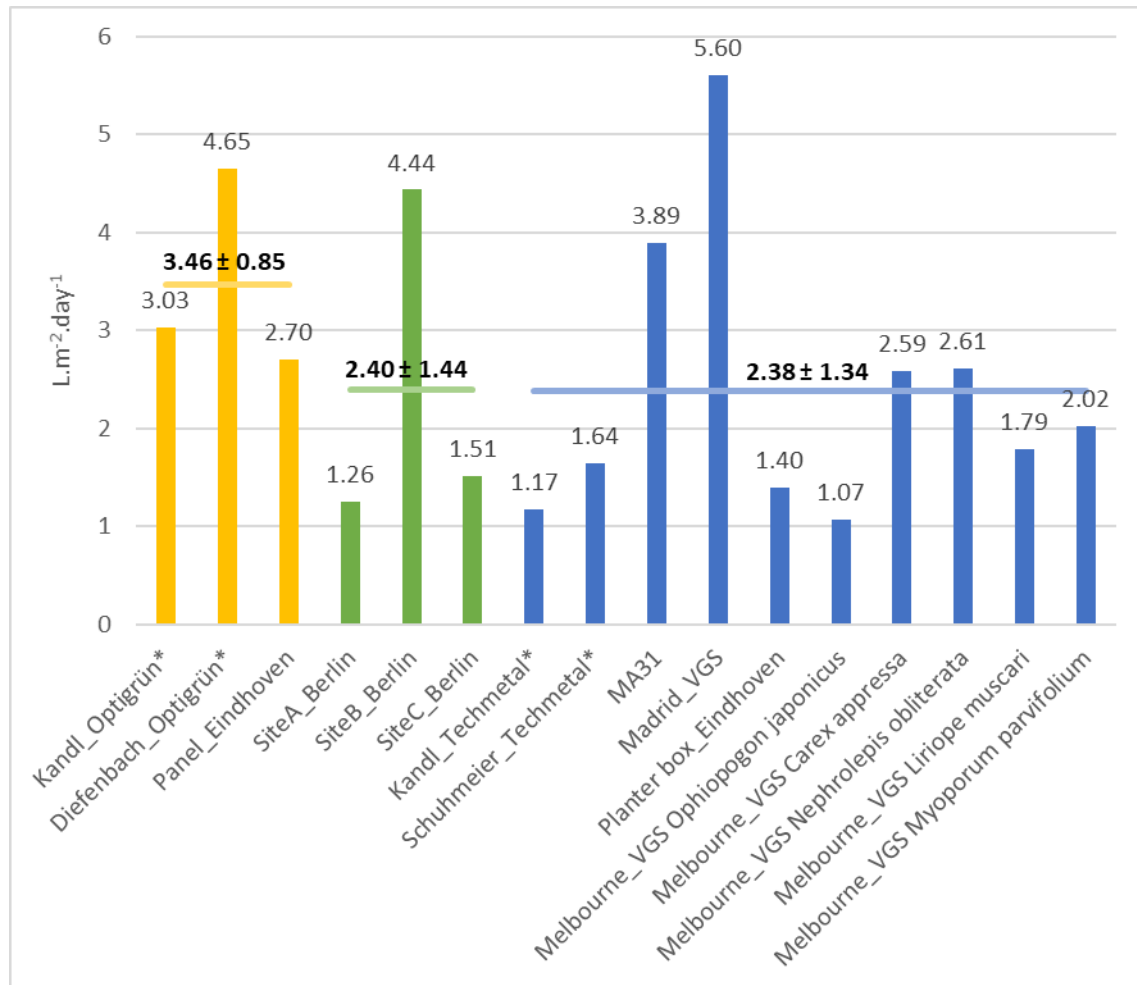


Figure 10: Daily water demand and irrigation amounts (marked with a star) per square meter greened area for continuous living walls (yellow), green facades (green) and modular living walls (blue).

The water demand and irrigation amounts per kilogram biomass and day are shown in Figure 11. Biomass data was not available for green facades, which is why the graph only shows continuous and modular living walls. With  $41.24 \pm 5.92 \text{ L.kg}^{-1}.\text{day}^{-1}$ , continuous living walls have a higher water demand/irrigation demand than modular living walls with  $10.46 \pm 6.44 \text{ L.kg}^{-1}.\text{day}^{-1}$ .

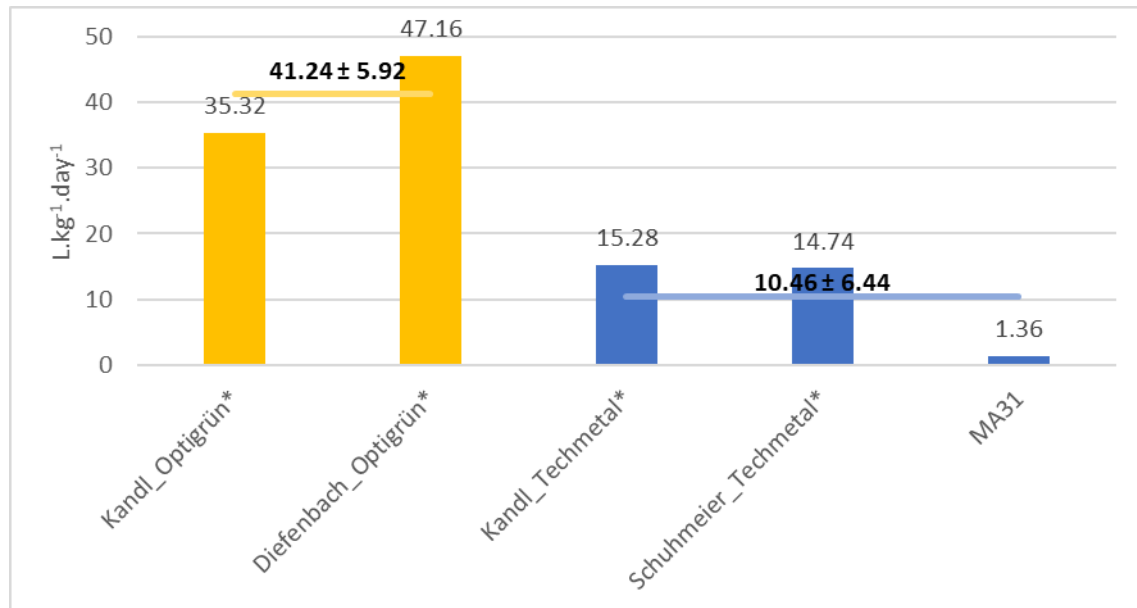


Figure 11: Daily water demand and irrigation amounts (marked with a star) per kilogram biomass on a summer day for continuous living walls (yellow) and modular living walls (blue).

Figure 12 shows the water demand and irrigation amounts per cubic meter substrate volume and day. The average water demand/irrigation amount and standard deviation are  $75.63$ ,  $57.05 \pm 14.82$  and  $21.12 \pm 31.01$  L.m<sup>-3</sup>.day<sup>-1</sup> for green facades, continuous living walls and modular living walls, respectively.

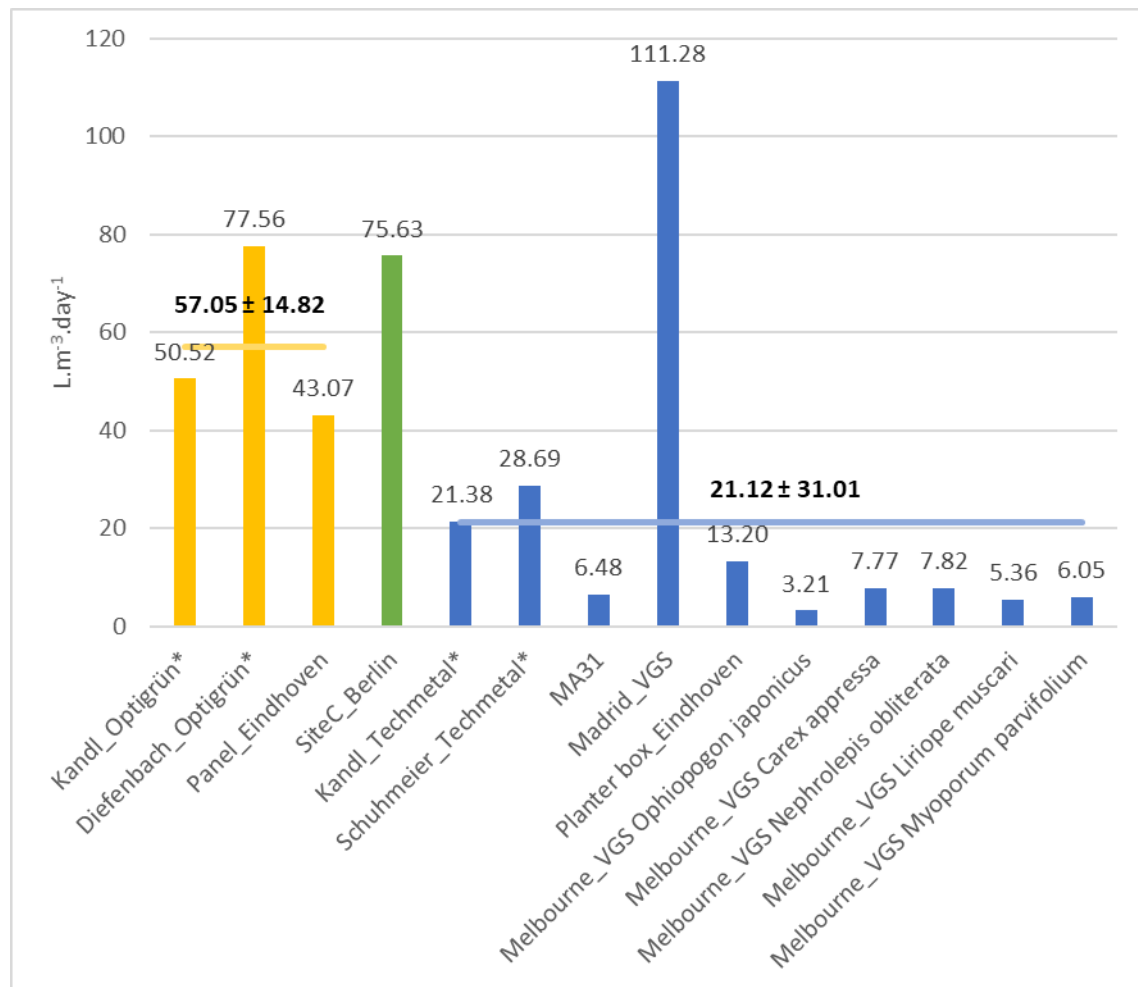


Figure 12: Daily water demand and irrigation amounts (marked with a star) per substrate volume on a summer day for continuous living walls (yellow), green facades (green) and modular living walls (blue).

### 5.2.2 Analysis of VGS characteristics

To explain the difference between the VGS types and their average annual water demand and irrigation amounts (Figure 9 and Figure 10), a closer look has to be taken at their characteristics. This chapter aims at comparing the substrate characteristics, the relative substrate volume, the greened area and the relative biomass to the daily water demand and irrigation amounts per square meter. Moreover, the plant characteristics of green facades are investigated to explain the water demand differences between SiteA\_Berlin, SiteB\_Berlin and SiteC\_Berlin (Figure 10).

Substrate characteristics were only available for four sites. Three modular living walls and one continuous living wall (Table 4). Interestingly, the comparison of MA31 and Madrid\_VGS shows that a higher water holding capacity does not result in a lower water demand. On the contrary, the comparison of Planter box\_Eindhoven and Panel\_Eindhoven shows that a higher water buffering capacity does result in a lower water demand. More comparable data would be needed to formulate general conclusions.

Table 4: Comparison of substrate characteristics and water demand of selected sites.

ID	VGS type	Substrate composition	Substrate characteristics	Water demand $\text{m}^3 \cdot \text{m}^{-2} \cdot \text{year}^{-1}$
MA31	Modular living wall	Granulite, expanded clay chippings, perlite, compost class A+	28.37% water holding capacity	0.50
Madrid_VGS	Modular living wall	Mixture of blond and black peat, coconut fibre, perlite, vermiculite, earthworm humus, and diatomite	46.89% water holding capacity 60.4% organic matter 88.1% total porosity 11.9% solid fraction	0.94
Planter box_Eindhoven	Modular living wall	Potting soil	High water buffering capacity	0.36
Panel_Eindhoven	Continuous living wall	Mineral wool	Low water buffering capacity	0.63

The relation of the total substrate volume to the daily water demand/irrigation amount per square meter is shown in Figure 13. In the left graph, the site MA31 sticks out very dominantly. To have a closer look at the distribution of the other sites, MA31 is removed in the right graph. From the graph it can be deduced that a higher substrate volume results in a lower demand per square meter.

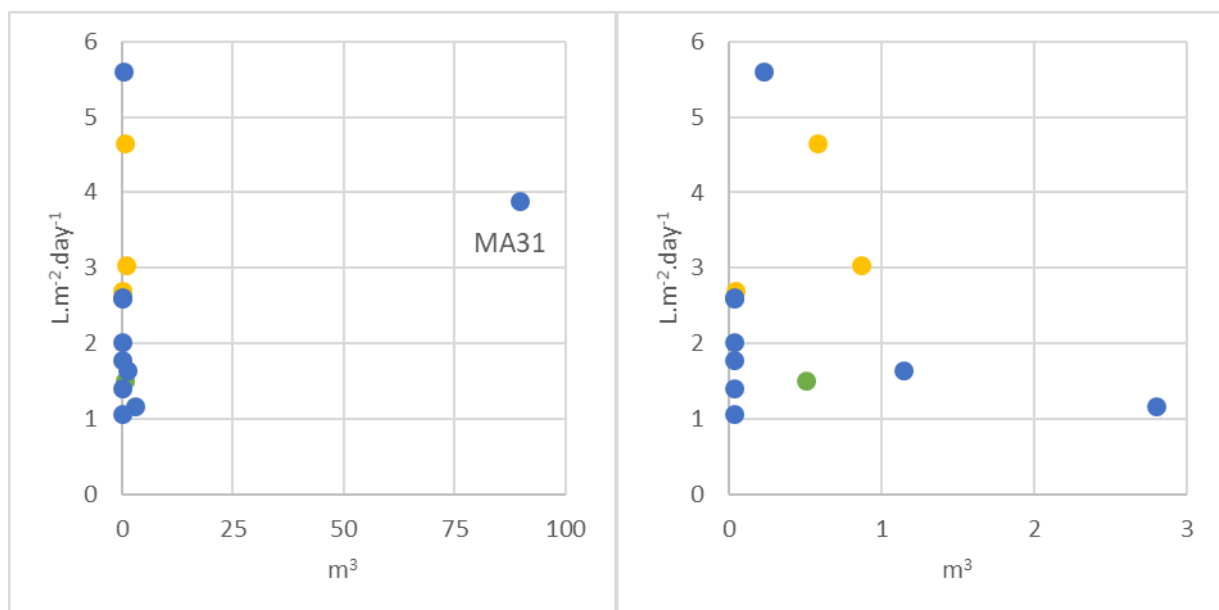


Figure 13: Total substrate volume plotted against the water demand/irrigation amount per square meter greened area on a summer day for continuous living walls (yellow), green facades (green) and modular living walls (blue). Left: without Mexico\_VGS, right: without Mexico\_VGS and MA31.

The relation of the relative substrate volume to the water demand/irrigation amounts per square meter for modular and continuous living walls is shown in Figure 14 and Figure 15. For the modular systems investigated, no relation is detectable with the data available. Without the site Mexico\_VGS, only three data points are available for the continuous living walls. For a similar relative substrate volume, all three systems have a different water demand. It has to be kept in mind that two of these three datapoints are irrigation amounts and not the actual plant water demand.

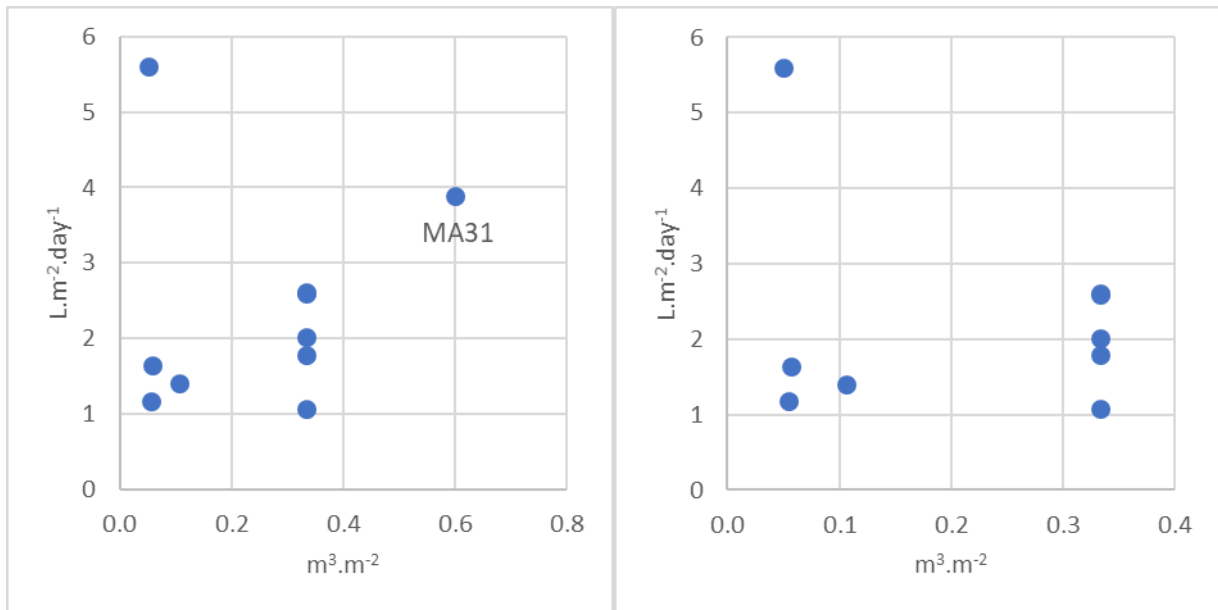


Figure 14: Water demand/irrigation amounts (\*) per  $m^2$  and relative substrate volume of modular living walls with (left) and without (right) MA31.

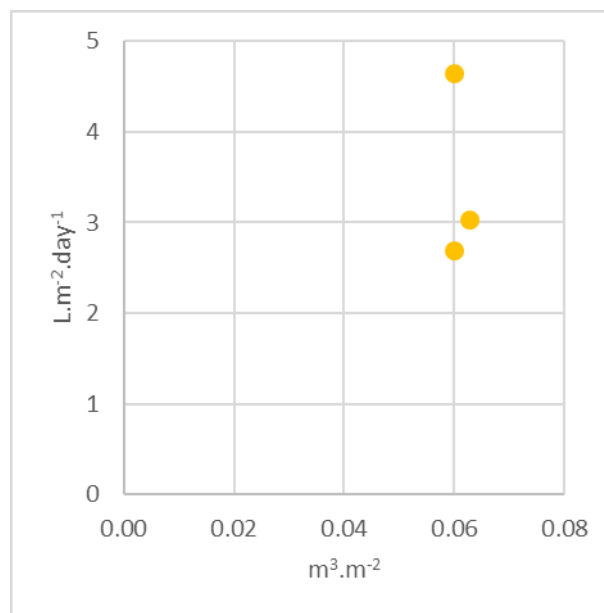


Figure 15: Water demand/irrigation amounts (\*) per  $m^2$  and relative substrate volume of continuous living walls without Mexico\_VGS.

Figure 16 shows the relation of the relative biomass to the daily water demand and irrigation amounts per kilogram biomass. The left graph clearly shows that compared to the others MA31 is a bigger greenery, needing a lot of water. After MA31 is removed, the right graph shows a clear distinction between continuous and modular living walls. The relative biomass for both systems is in the same range. However, continuous systems need a higher water amount per kilogram biomass than modular systems.

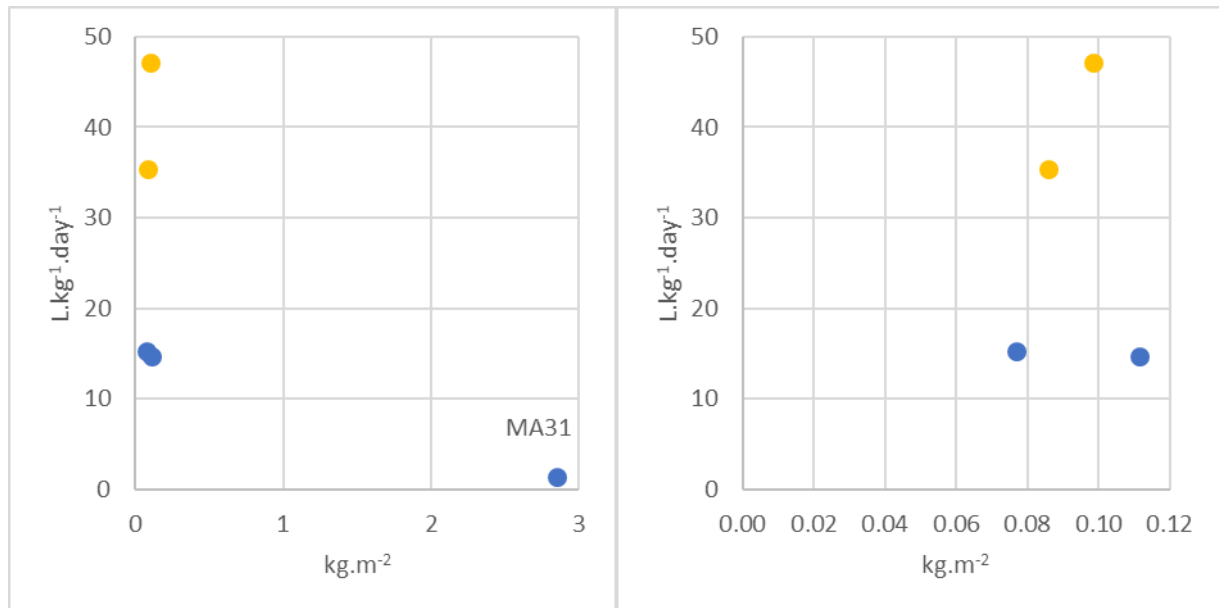


Figure 16: Relative biomass plotted against the daily water demand and irrigation amounts per kilogram biomass for a summer day for continuous living walls (yellow) and modular living walls (blue) with (left) and without (right) MA31.

Figure 10 shows high differences in water demand between SiteA\_Berlin, SiteB\_Berlin and SiteC\_Berlin. As the substrate volume and composition are assumed to be similar, the plant characteristics of the green facades might be a reason for the difference. However, the differences cannot be explained with the WLAI, which is 1.9 for SiteA\_Berlin and 3.0 for SiteB\_Berlin and SiteC\_Berlin (Hoelscher, 2018). Hence, SiteB\_Berlin and SiteC\_Berlin would have to have similar water demands. Therefore, the difference in water demand of those two sites might result from plant-physiological characteristics of *Hedera helix* (SiteB\_Berlin) and *Fallopia baldschuanica* (SiteC\_Berlin), which influence the transpiration rate (compare Chapter 3.2.2). This statement is supported by the results from Prodanovic *et al.* (2019), who showed different responses of plant species to the same environment.

The relation between the greened area and the daily water demand and irrigation amounts per square meter is shown in Figure 17. From the graph, it can be concluded that for bigger VGS, the water demand per square meter is lower than for smaller VGS.



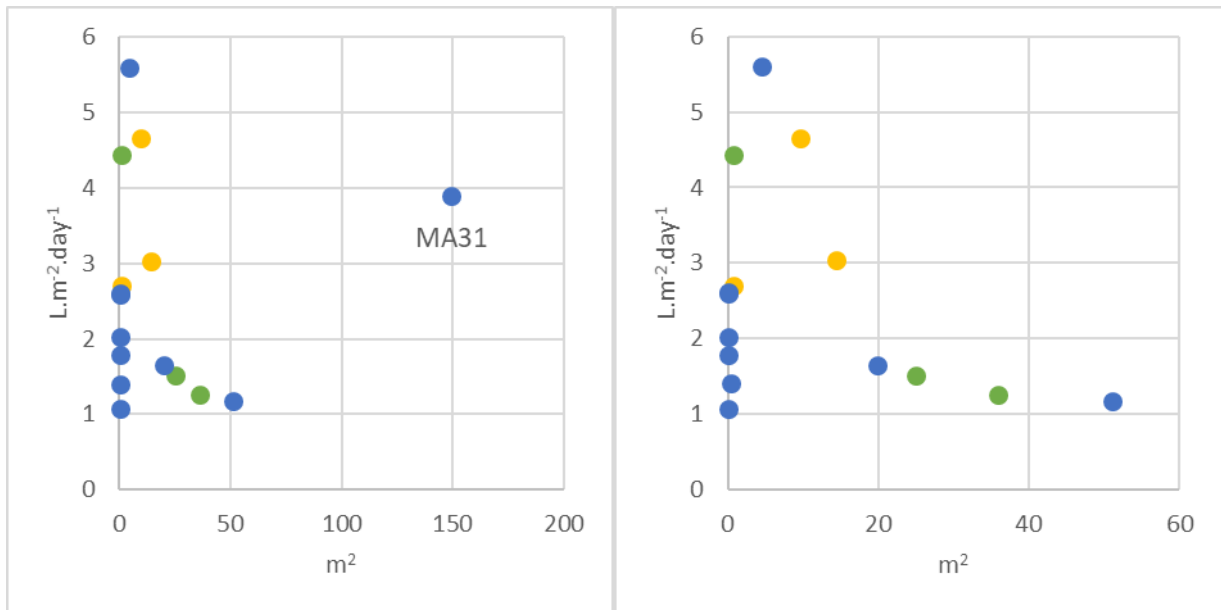


Figure 17: Greened area plotted against the water demand/irrigation amount for a summer day for continuous living walls (yellow), green facades (green) and modular living walls (blue) with (left) and without (right) MA31.

Figure 18 shows the comparison of the total greened area in square meters. With  $81.46 \pm 106.16$  m<sup>2</sup>, green facades have the biggest average area of the sites investigated, followed by modular systems with  $22.56 \pm 45.01$  m<sup>2</sup> and continuous living walls with  $8.22 \pm 5.69$  m<sup>2</sup>.

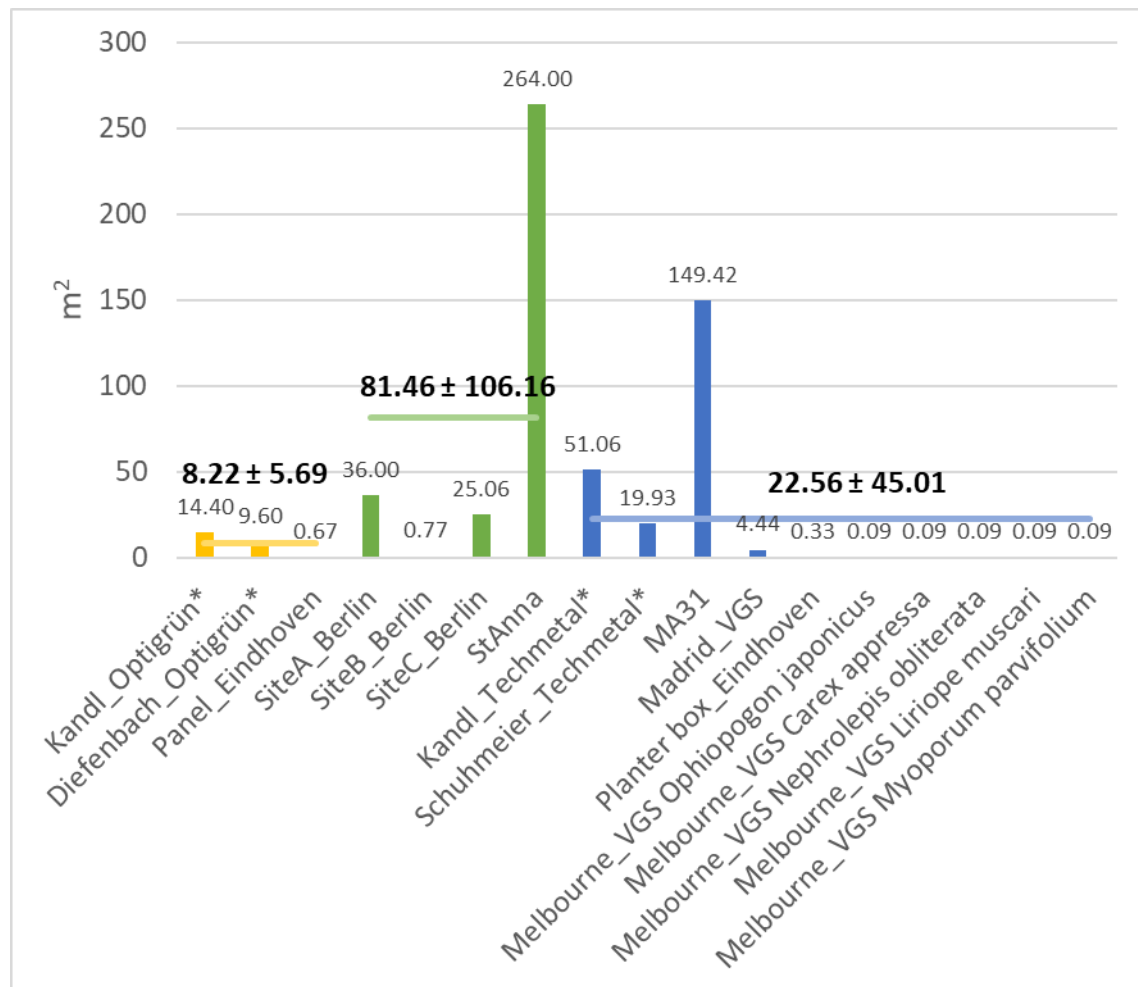


Figure 18: Total greened area in square meters for continuous living walls (yellow), green facades (green) and modular living walls (blue).

### 5.2.3 Discussion of database results

In this chapter the results of the water demand analysis are discussed.

The database was set-up based on the available data. Only few authors provided additional data on the measured water balance components, substrate characteristics, additional weather data, the course of the greened area and the plant biomass (Table 5). With this information, further impact factors on the water demand of VGS can be analysed. Especially, the effect of the substrate characteristics and the biomass on the water demand are of great interest and should be investigated in future research. Furthermore, more data on the course of the green coverage throughout the season would have delivered more accurate results of the water demand/ irrigation amount per square meter greened area. The course of the greened area could only be respected for 11 of 18 sites, otherwise a constant value for the greened area was used for the calculation. This assumption does not correspond to the growth period of plants. Figure 19 shows the resulting error for SiteC\_Berlin from using a constant greened area for the estimation of the water demand per square meter. In this example, the water demand per square meter is underestimated for the spring months.

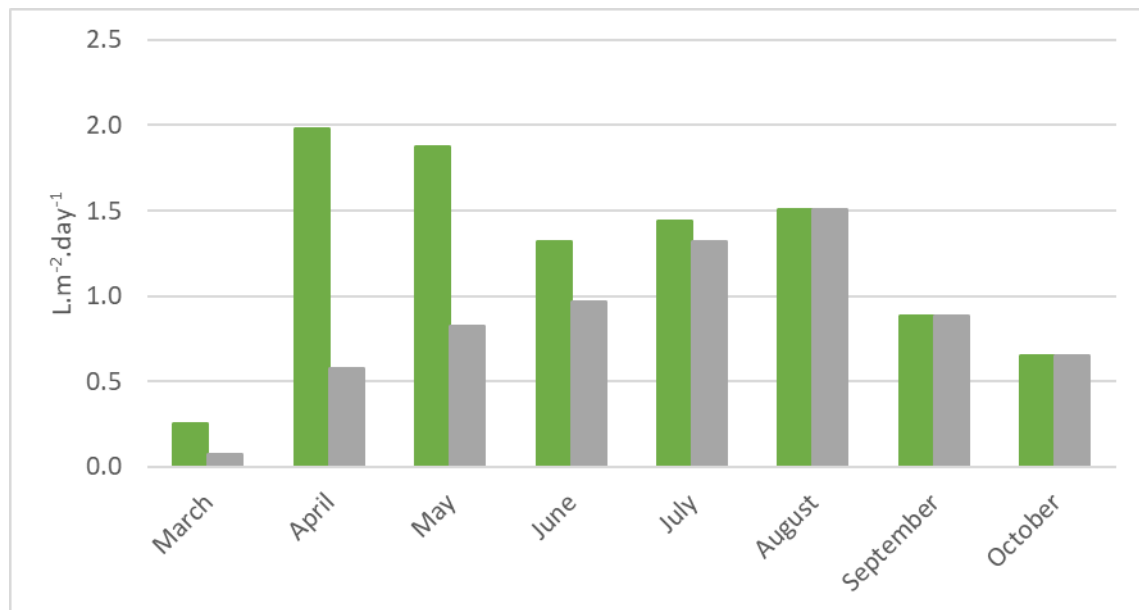


Figure 19: Comparison of the water demand per square meter for SiteC\_Berlin, calculated with the course of the greened area (green) and with a constant greened area of 25 m<sup>2</sup> (grey).

Table 5: Available information in the database.

ID	Water balance components	Substrate characteristics	Weather data	Course of greened area	<i>Total biomass</i> kg
Kandl_ Techmetal	-	-	-	No	3920.34
Schuhmeier_ Techmetal	-	-	-	No	2222.55
MA31	ET	28.37 % water holding capacity	-	No	425914.12
Madrid_VGS	ET	221 kg.m <sup>-3</sup> substrate bulk density, 46.89% Water holding capacity, 60.4% organic matter, 88.1% total porosity, 11.9% solid fraction	Precipitation	Yes	-
Planter box_ Eindhoven	Precipitation, ET, water balance flow chart with all components in percent	High water buffering capacity	Temperature, relative humidity, global radiation, precipitation	Yes	-
Melbourne_ VGS (5 different species)	Evaporation (monthly min and max values), transpiration for 5 different plant types (monthly min and max values)	-	Temperature	Yes	-
Kandl_ Optigrün	-	-	-	No	1235.57
Diefenbach_ Optigrün	-	-	-	No	947.27
Mexico_VGS	-	-	Precipitation, solar radiation, relative humidity, temperature	No	-
Panel_ Eindhoven	Precipitation, ET, water balance flow chart with all components in percent	-	Temperature, relative humidity, global radiation, precipitation	Yes	-
Site A_Berlin	Transpiration	-	Incoming short-wave radiation, air temperature, relative humidity	Yes	-
Site B_Berlin	Transpiration	-	Incoming short-wave radiation, air temperature, relative humidity	Yes	-
Site C_Berlin	Evaporation, Transpiration	-	Incoming short-wave radiation, outgoing long-wave radiation, wind speed, relative humidity, air temperature	Yes	-
StAnna	-	Low water buffering capacity	-	No	-

Several of the graphs (Figure 13, Figure 16, Figure 17, Figure 18) in the database analysis show that the site MA31 has an especially high relative substrate volume and relative biomass. Table 6 shows the comparison of the greened area, the relative substrate volume and the relative biomass of the VGS investigated. From the data available, MA31 shows to have the highest values compared to the other sites. The reason for these high values is the difference in system design of the VGS sites. Still, MA31 is not handled as an outlier in the analysis. However, for the

interpretation of the results it should be kept in mind that the average water demand values calculated for modular living walls is influenced.

Table 6: Greened area, relative substrate volume and relative biomass of the VGS investigated.

ID	<i>Greened area</i> m <sup>2</sup>	<i>Relative substrate volum</i> m <sup>3</sup> . m <sup>-2</sup>	<i>Relative biomass</i> kg. m <sup>-2</sup>
Kandl_Techmetal	51.06	0.05	0.08
Schuhmeier_Techmetal	19.93	0.06	0.11
MA31	149.42	0.60	2.85
Madrid_VGS	4.44	0.05	-
Planter box_Eindhoven	0.33	0.11	-
Melbourne_VGS	0.09	0.33	-
Kandl_Optigrün	14.40	0.06	0.09
Diefenbach_Optigrün	9.60	0.06	0.10
Mexico_VGS	5.46	0.05	-
Panel_Eindhoven	0.67	0.06	-
Site A_Berlin	36	-	-
Site B_Berlin	0.77	-	-
Site C_Berlin	25.06	0.02	-
StAnna	264	-	-

The results obtained from the analysis of the database can be used for the planning of future VGS. Generally, the irrigation management has to be efficient with a minimal irrigation amount to reduce operational costs. However, the goal of a minimal irrigation amount should not compromise the VGS ecosystem services. The plants' ability to contribute to e.g. cooling of the surrounding air, improvement of air quality and noise reduction (see Figure 2) does depend on the plants' health where an optimal water supply plays a crucial role. Depending on the pursued purpose of the VGS implementation, a different type of VGS will be chosen. If the goal is to reduce the urban temperature, ET and shading are two of the main contributors to providing this function (Hoelscher *et al.*, 2016). The assumption is that a high ET rate and shading effect come along with a high plant biomass and high water demand. Therefore, the water demand per kilogram biomass is of highest interest. Figure 15 shows that continuous living walls have a higher water demand per square meter and kilogram biomass than modular living walls. Based on this database analysis it can be concluded that continuous living walls are more suitable for the cooling of surrounding air than modular living walls. If the goal of the VGS installation is an increase in urban biodiversity, a big greenery with a low water demand is assumed to be optimal. In this case, the water demand per greened area is most relevant. Figure 8 shows that green facades have the lowest water demand per greened area compared to modular and continuous living walls. Hence, the results of this database analysis hint at green facades being the best choice for increasing biodiversity in the urban surrounding. However, it should be kept in mind that these recommendations are based on the assumptions mentioned. Future research is needed to investigate the effect of VGS features (plants, substrate, greened area, type) on the contribution to ecosystem service. This would allow improved recommendations for the selection of VGS type for different purposes.

A closer look was taken at the results of the water demand analysis (Chapter 5.2.1). The results show that depending on the reference chosen (greened area, biomass, substrate volume), the order of the VGS type with the highest water demand changes. Based on the analysis of VGS characteristics (Chapter 5.2.2), the following paragraphs describe possible explanations for these differences.

The water demand per square meter greened area (Figure 10) is highest for continuous living walls, followed by modular living walls and green facades. These differences between the VGS types can be explained with the size difference of the VGS investigated. Figure 18 shows that of the sites investigated, green facades have the biggest greened area, followed by modular and continuous systems. As shown in Figure 17, a bigger greened area results in a lower water demand per greened area. Hence, the analysis of the water demand shows that VGS with the smallest greened area (continuous living walls) have the highest water demand per square meter greened area.

The water demand per kilogram biomass (Figure 11) is highest for continuous living walls, followed by modular living walls. This is also shown in Figure 16. Although the relative biomass of the continuous and modular systems analysed are in the same range, the water demand per kilogram biomass is higher for continuous living walls than for modular living walls. A possible explanation for these differences are the plant-physiological characteristics. Prodanovic *et al.* (2019) conducted experiments to investigate the water demand of different plant species. Their results show that every plant species has a specific water demand for the same environmental conditions.

Figure 12 shows that the water demand per substrate volume is highest for green facades, followed by continuous living walls and is least for modular systems. In this analysis the substrate volume of one green facade was respected due to lack of data, which is why this value is not further discussed. However, the difference between continuous and modular living walls can be explained by the differences in substrate characteristics. Van de Wouw *et al.* (2017) mention the lower water buffering capacity of mineral wool as one reason for the higher irrigation amount in continuous green walls. The authors argue that the capillary rise in mineral wool used in continuous systems is a magnitude lower than the capillary rise of modular systems (0.5 m). Therefore, the upper parts in continuous living walls is deprived of water and needs constant replacement. As shown in Table 5, data on the substrate characteristics is available for 4 out of 18 greeneries investigated. If available, it is recommended to publish this data in future papers on VGS related topics to allow the further use of already existing data in other research projects.

The analysis of the water demand shows that the comparison of annual water demand per greened area (Figure 9) shows different results than the comparison of the daily water demand per greened area (Figure 10). In both comparisons, continuous living walls have the highest demand. However, the second and third place of the ranking are different. In the annual comparison, modular systems have a significantly higher demand than green facades. In the daily comparison, modular systems and green facades have a very similar demand. This difference might result from the different data available for the respective analysis. The same amount of data was available for continuous and modular living walls. However, the annual comparison of green facades was done with one value and the daily comparison with three values. This results in a different ranking of the water demand per square meter greened area.

Last, the values for water demand and irrigation amounts were derived from different measurement methods (Table 2) namely the irrigation amount with and without soil humidity sensors, sap flow measurements, lysimeter measurements and ET rates derived by a water balance approach. To distinguish between these methods, the data has been declared as water demand or irrigation amount. The analysis is based on the assumption that the comparability of these methods is given. However, the comparability of these methods is limited. The comparison could be improved with the provision of more data on the water balance components (ET, the drainage, the irrigation and precipitation amounts).

### 6. Conclusions

Within this Master's thesis, the calculation of the optimal irrigation amount of VGS was investigated. To provide possible solutions for a sustainable irrigation with rainwater, RWH scenarios were elaborated.

The calculation of the optimal irrigation amount was based on a conceptual model (Figure 20). The model visualises the hydrological processes in VGS, which allows the calculation of the optimal irrigation amount. The following conclusions can be drawn regarding the optimal irrigation amount:

1. The optimal irrigation amount is dependent on the soil water content. If the soil water content drops below the RAW, additional water input via irrigation is necessary.
2. The soil water content is changed by the inflows and outflows to the system, which are ET, collected precipitation, run-on from surrounding areas, overflow from the system and percolation through the drainage.
3. The three types of VGS have different designs, which results in changes of the inflows and outflows. For the calculation of the irrigation demand, the boundary conditions for each type have to be considered.

More knowledge about the irrigation demand of VGS was created with the VGS database. For the database, 18 greeneries from around the world have been collected. Information about their characteristics have been added to be able to compare their water demands. The analysis of the database allows the following conclusions:

1. Continuous living walls have the highest annual water demand per greened area with  $3.46 \pm 0.85 \text{ L.m}^{-2}.\text{day}^{-1}$ , followed by modular living walls with  $2.40 \pm 1.44 \text{ L.m}^{-2}.\text{day}^{-1}$  and green facades with  $2.38 \pm 1.34 \text{ L.m}^{-2}.\text{day}^{-1}$  (Figure 10).
2. Green facades have the highest daily water demand per substrate volume with  $75.63 \text{ L.m}^{-3}.\text{day}^{-1}$ , followed by continuous living walls with  $57.05 \pm 14.82 \text{ L.m}^{-3}.\text{day}^{-1}$  and modular living walls with  $21.12 \pm 31.01 \text{ L.m}^{-3}.\text{day}^{-1}$  (Figure 12).
3. Continuous living walls have a higher water demand per kilogram biomass with  $41.24 \pm 5.92 \text{ L.kg}^{-1}.\text{day}^{-1}$  than modular living walls with  $10.46 \pm 6.44 \text{ L.kg}^{-1}.\text{day}^{-1}$  (Figure 11).
4. This information helps with the choice of VGS type for future projects. Depending on the aim of a VGS installation (support of urban biodiversity vs. improvement of urban microclimate), a type with a higher or lower water demand has to be chosen.
5. A higher total substrate volume results in a lower water demand per square meter greened area (Figure 13).
6. The reason for the difference in water demand between continuous and modular living walls are a lower substrate volume and higher water demand per kg biomass in continuous systems.
7. For modular living walls, no trend can be detected between the water demand ( $\text{L.m}^{-2}.\text{day}^{-1}$ ) and relative substrate volume ( $\text{m}^3.\text{m}^{-2}$ ).

## Conclusions

---

8. For continuous living walls, there is a slight trend of a higher relative substrate volume ( $\text{m}^3.\text{m}^{-2}$ ) resulting in a lower water demand ( $\text{L}.\text{m}^{-2}.\text{day}^{-1}$ ).
9. The location influences the water demand as VGS located in an arid climate have a significantly higher water demand than VGS located in temperate or cold climate.

Furthermore, the conceptual model is the basis for the RWH scenarios. Depending on the characteristics of the surrounding, different tank positions, run-off surfaces and treatment facilities have to be chosen. The following conclusions can be drawn regarding RWH for the irrigation of VGS:

1. In urban areas with low building density and degree of development, RWH on a building scale with harvesting of roof run-off is recommended.
2. In urban areas with high building density and degree of development, RWH on a building scale or on the block scale is recommended. Run-off from roof and street surfaces can be used for irrigation.
3. Run-off from roof areas with a low pollution rate can be treated by mechanical filtration and sedimentation.
4. Run-off from street areas with a high pollution rate must be treated better, e.g. by a sediment grit chamber, a biological treatment with a planted substrate filter and a subsequent UV disinfection.



## 7. Summary and outlook

VGS are effective instruments to help modern cities adapt to the effects of climate change. Plants cool their environment by transpiration and shading and can therefore improve the surrounding microclimate. However, this positive function can only be provided if the plant is supplied with enough water. Hence, an optimal irrigation amount is required to reduce water losses due to over-irrigation. Additional to an optimal irrigation amount, the source of irrigation water has to be considered. With an increase in population and an on-going urbanisation process, no additional pressure should be put on drinking water resources. Therefore, alternative resources such as rainwater should be chosen.

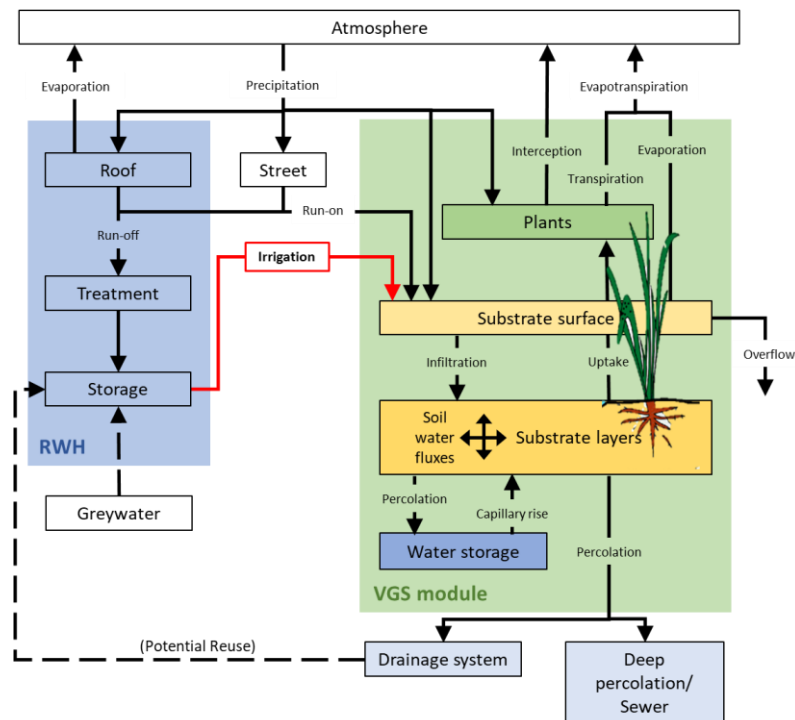


Figure 20: Conceptual model.

Water demand as well as supply are essential parts of the operation of VGS. The first research objective of the thesis was to provide a conceptual model to calculate the water demand of VGS. The conceptual model was created based on the water balance, representing the prevailing hydrological processes in VGS. The water demand was calculated via the soil water content. If the soil water content drops below FC, additional water input via irrigation is necessary. The changes in soil water content are due to in- and outflows of water to and from the VGS. These flows are described with selected equations. Since the aim of this thesis was to describe the water demand calculation of VGS with formulas, a calibration and validation of the model was not performed. This testing of the model exceeds the extent of this thesis, but would be recommended for future research.

In addition to the conceptual model, a VGS database was set up to gather further knowledge about the water demand of VGS. The database contains 18 greeneries from around the world. Information about water and irrigation amounts, system design, planting and location has been gathered. The information was used first, to compare the water demand and irrigation amounts of the three VGS types, and second to find possible explanations of the differences in water demand. The results have shown that continuous living walls have the highest annual water demand or irrigation amount per square meter greened area, followed by modular living walls and green facades (Figure 9). If the water demand and irrigation amount per square meter on a summer day are compared, the order changes (Figure 10). Continuous living walls still have the highest water demand per greened area. However, modular living walls and green facades have

a very similar water demand. This difference is expected to result from the data basis available for the two comparisons. For the annual water demand, data was only available for one green facade (StAnna), while data for the analysis of the water demand on a summer day was available for three green facades (SiteA\_Berlin, SiteB\_Berlin and SiteC\_Berlin). Looking at the water demand per cubic meter substrate volume, green facades have shown to have the highest demand, followed by continuous and modular living walls. The comparison of the water demand per kilogram biomass shows that continuous living walls have a higher demand than modular living walls.

Furthermore, the information on system design, planting and location was used to analyse the obtained water demands and irrigation amounts. One site (Mexico\_VGS) had to be removed as an outlier because the location in an arid climate resulted in a very high annual water demand compared to the other sites. The system design was investigated by comparing the substrate characteristics and volume of the sites. The substrate characteristics have not shown to result in trends in water demand, which might be due to the scarce data basis available. For future research, it would be recommendable to gather more information of the substrate characteristics and analyse the influence on water demand of VGS. The substrate volume was analysed and proved to have an impact on the water demand. From the data available it can be concluded that a higher total substrate volume results in a lower water demand per square meter per day. The planting was analysed using the kilograms biomass growing on the VGS. The results suggest that continuous living walls have a higher water demand per kilogram biomass than modular living walls. However, only 4 VGS were compared for this analysis. From this data, no conclusion can be drawn on the magnitude of influence on the water demand resulting from biomass. A more detailed calculation of the biomass of the sites, also considering the annual change of biomass, and subsequent comparison of water demands are therefore recommendable.

Setting up the database revealed the lack of information on the water demand and VGS characteristics. It is therefore suggested that future research on this topic includes as much detailed information as possible of the measured water balance components, the substrate characteristics, the system geometry, the plant type, the biomass, the changes of the greened area throughout the year and local weather and climate. This information would allow a more thorough comparison of the systems and help to foster the understanding of the influences on VGS water demand.

The second research question of this thesis dealt with the provision of irrigation water from RWH. This question was answered with the conceptual model. The calculation of the RWH amount is based on the rational method and was presented with the governing equations of the model. Furthermore, two RWH scenarios were elaborated based on two different structure types with a high and low degree of development and high building density. Scenario A for a low degree of development and building density represents a suburban environment with single-family houses. It is suggested to collect rainwater from roof areas and store the water on the building scale either in a tank distributed over the roof or an underground tank. A collection of water from the street surfaces is not recommended due to a higher pollution level. The roof run-off needs to be treated by mechanical filtration and sedimentation only due to the low pollution level. Scenario B describes the RWH for a high degree of development and building density, as can be found in city centres. The rainwater can be harvested from roof and street areas. The water can be stored either on a building scale (tank distributed over the roof) or on the block scale (in a block tank). The treatment needs to be more elaborated due to the higher pollution of street areas. One suggested treatment is a sediment grit chamber, a biological treatment with a planted substrate filter and a subsequent UV disinfection.

In conclusion, this thesis provided a conceptual model to calculate the water demand of VGS and to estimate the run-off collectable from RWH. Furthermore, the model helped to establish the RWH scenarios. In addition, a VGS database was created to give more insight into their characteristics and the influence of these characteristics on the water demand.

## 8. References

- Abbasi, T., Abbasi, S.A. (2011) Sources of Pollution in Rooftop Rainwater Harvesting Systems and Their Control. *Critical Reviews in Environmental Science and Technology*. **41**(23), 2097–2167.
- Allen, R.G., Pereira, L.S., Raes, D., Smith, M. (1998) *Crop evapotranspiration. Guidelines for computing crop water requirements - FAO Irrigation and drainage paper 56*. Rome: Food and Agriculture Organization of the United Nations.
- Amelung, W., Blume, H.-P., Fleige, H., Horn, R., Kandeler, E., Kögel-Knabner, I., Kretzschmar, R., Stahr, K., Wilke, B.-M. (2018) Physikalische Eigenschaften und Prozesse. In *Scheffer/Schachtschabel Lehrbuch der Bodenkunde*. Berlin, Heidelberg: Springer Berlin Heidelberg, pp. 213–340.
- Angrill, S., Farreny, R., Gasol, C.M., Gabarrell, X., Viñolas, B., Josa, A., Rieradevall, J. (2012) Environmental analysis of rainwater harvesting infrastructures in diffuse and compact urban models of Mediterranean climate. *The International Journal of Life Cycle Assessment*. **17**(1), 25–42.
- Bustami, R.A., Belusko, M., Ward, J., Beecham, S. (2018) Vertical greenery systems: A systematic review of research trends. *Building and Environment*. **146**, 226–237.
- Depietri, Y., McPhearson, T. (2017) Integrating the Grey, Green, and Blue in Cities: Nature-Based Solutions for Climate Change Adaptation and Risk Reduction. In N. Kabisch, H. Korn, J. Stadler, & A. Bonn, eds. *Nature-based Solutions to Climate Change Adaptation in Urban Areas. Linkages between Science, Policy and Practice*. Springer Open, pp. 91–109.
- Dingman, S.L. (2015) *Physical hydrology*. Third Edit. Long Grove, Illinois: Waveland Press.
- EC DG (2015) Towards an EU Research and Innovation policy agenda for Nature-Based Solutions & Re-Naturing Cities. Final Report of the Horizon 2020 Expert Group on ‘Nature-Based Solutions and Re-Naturing Cities’ (full version). [online]. Available from: <https://publications.europa.eu/en/publication-detail/-/publication/fb117980-d5aa-46df-8edc-af367cddc202> [Accessed March 18, 2019].
- Emilsson, T., Ode Sang, Å. (2017) Impacts of Climate Change on Urban Areas and Nature-Based Solutions for Adaptation. In N. Kabisch, H. Korn, J. Stadler, & A. Bonn, eds. *Nature-based Solutions to Climate Change Adaptation in Urban Areas. Linkages between Science, Policy and Practice*. Springer Open, pp. 15–27.
- Environment Agency (2010) *Harvesting rainwater for domestic uses: an information guide*. Bristol: Environment Agency.
- Enzi, V., Cameron, B., Dezsényi, P., Gedge, D., Mann, G., Pitha, U. (2017) Nature-Based Solutions and Buildings – The Power of Surfaces to Help Cities Adapt to Climate Change and to Deliver Biodiversity. In N. Kabisch, H. Korn, J. Stadler, & A. Bonn, eds. *Nature-based Solutions to Climate Change Adaptation in Urban Areas. Linkages between Science, Policy and Practice*. Springer Open, pp. 159–183.
- Ertl, T., Fürhacker, M., Pitha, U., Allabashi, R., Scharf, B., Measho, H.T. (2016) *Straßen Abwasserlösungen für Vegetation und Entwässerung SAVE*.
- EU (2006) Badegewässerrichtlinie - Richtlinie 2006/7/EG des europäischen Parlaments und des Rates vom 15. Februar 2006 über die Qualität der Badegewässer und deren Bewirtschaftung und zur Aufhebung der Richtlinie 76/160/EWG.
- Farreny, R., Morales-Pinzón, T., Guisasola, A., Tayà, C., Rieradevall, J., Gabarrell, X. (2011) Roof selection for rainwater harvesting: Quantity and quality assessments in Spain. *Water Research*. **45**(10), 3245–3254.

## References

---

- Feng, Y. (2019) Evapotranspiration from Green Infrastructure: Benefit, Measurement, and Simulation. In D. Bucur, ed. *Advanced Evapotranspiration Methods and Applications*. IntechOpen, p. 13.
- Forzieri, G., Feyen, L., Russo, S., Voutsdoukas, M., Alfieri, L., Outten, S., Migliavacca, M., Bianchi, A., Rojas, R., Cid, A. (2016) Multi-hazard assessment in Europe under climate change. *Climatic Change*. **137**(1–2), 105–119.
- Givoni, B. (1991) Impact of planted areas on urban environmental quality: A review. *Atmospheric Environment. Part B. Urban Atmosphere*. **25**(3), 289–299.
- Grimm, N.B., Faeth, S.H., Golubiewski, N.E., Redman, C.L., Wu, J., Bai, X., Briggs, J.M. (2008) Global Change and the Ecology of Cities. *Science*. **319**(5864), 756–760.
- GrüneZukunftSchule (2018) *Grün im Schulneubau – Living Wall Systemvorstellung*.
- GrünPlusSchule (2018) *Ein Maßnahmenkatalog für die Begrünung von Schulen im Altbau anhand des Beispiels Gymnasium und Realgymnasium 7, Kandlgasse 39, 1070 Wien*.
- Haines, A., Kovats, R.S., Campbell-Lendrum, D., Corvalan, C. (2006) Climate change and human health: Impacts, vulnerability and public health. *Public Health*. **120**(7), 585–596.
- Herrera, J., Bonilla, C.A., Castro, L., Vera, S., Reyes, R., Gironás, J. (2017) A model for simulating the performance and irrigation of green stormwater facilities at residential scales in semiarid and Mediterranean regions. *Environmental Modelling & Software*. **95**, 246–257.
- Herrera, J., Flamant, G., Gironás, J., Vera, S., Bonilla, C., Bustamante, W., Suárez, F. (2018) Using a Hydrological Model to Simulate the Performance and Estimate the Runoff Coefficient of Green Roofs in Semiarid Climates. *Water*. **10**(2), 198.
- Hoelscher, M.-T., Nehls, T., Jänicke, B., Wessolek, G. (2016) Quantifying cooling effects of facade greening: Shading, transpiration and insulation. *Energy and Buildings*. **114**, 283–290.
- Hoelscher, M. (2018) *Quantification of cooling effects and water demand of urban facade greenings*. Technical University of Berlin.
- Hopkins, G., Goodwin, C. (2011) *Living Architecture: Green Roofs and Walls*. Collingwood VIC: CSIRO Publishing.
- International Society of Soil Science (1952) Bulletin No. 49.
- Köhler, M. (2008) Green facades—a view back and some visions. *Urban Ecosystems*. **11**(4), 423–436.
- Manso, M., Castro-Gomes, J. (2015) Green wall systems: A review of their characteristics. *Renewable and Sustainable Energy Reviews*. **41**, 863–871.
- Marasco, D. (2014) *Alternative Metrics of Green Roof Hydrologic Performance: Evapotranspiration and Peak Flow Reduction*. Columbia University, New York, NY, USA.
- Matzinger, A., Riechel, M., Remy, C., Schwarzmüller, H., Rouault, P., Schmidt, M., Offermann, M., Strehl, C., Nickel, D., Sieker, H., Pallasch, M., Köhler, M., Kaiser, D., Möller, C., Büter, B., Leßmann, D., von Tils, R., Säumel, I., Pille, L., Winkler, A., Bartel, H., Heise, S., Heinzmann, B., Joswig, K., Rehfeld-Klein, M., Reichmann, B. (2017) *Zielorientierte Planung von Maßnahmen der Regenwasserbewirtschaftung - Ergebnisse des Projektes KURAS*. Berlin.
- Mobilia, M., Longobardi, A., Sartor, J. (2017) Including A-Priori Assessment of Actual Evapotranspiration for Green Roof Daily Scale Hydrological Modelling. *Water*. **9**(2), 72.
- NOAA National Centers for Environmental Information State of the Climate (2019) Global Climate Report for July 2019. [online]. Available from: <https://www.ncdc.noaa.gov/sotc/global/201907> [Accessed December 30, 2019].
- Nolde, E. (2007) Possibilities of rainwater utilisation in densely populated areas including precipitation runoffs from traffic surfaces. *Desalination*. **215**(1–3), 1–11.

## References

---

- ÖNORM EN 16941-1 (2018) *On-site non-potable water systems - Part 1: Systems for the use of rainwater*.
- ÖWAV-Regelblatt 35 (2019) Einleitung von Niederschlagswasser in Oberflächengewässer.
- ÖWAV-Regelblatt 45 (2015) *Oberflächenentwässerung durch Versickerung in den Untergrund*. Wien: Österreichischer Wasser- und Abfallwirtschaftsverband.
- Peel, M.C., Finlayson, B.L., McMahon, T.A. (2007) Updated world map of the Köppen-Geiger climate classification. *Hydrology and Earth System Sciences*. **11**, 1633–1644.
- Pelko, C. (2018) *Vertikaler Garten in Wien. Monitoring der Fassadenbegrünung am Amtsgebäude der MA31*. Universität für Bodenkultur.
- Pfoser, N., Jenner, N., Henrich, J., Heusinger, J., Weber, S. (2013) *Gebäude, Begrünung und Energie: Potenziale und Wechselwirkungen*.
- Pitha, U., Scharf, B., Enzi, V., Oberarzbacher, S., Hancvencl, G., Wenk, D., Steinbauer, G., Oberbichler, C., Lichtblau, A., Erker, G., Fricke, J., Haas, S., Preiss, J. (2013) *Leitfaden Fassadenbegrünung*. Vienna.
- Priestley, C.H.B., Taylor, R.J. (1972) On the assessment of surface heat flux and evaporation using large-scale parameters. *Monthly Weather Review*. (100), 81–92.
- Prodanovic, V., Wang, A., Deletic, A. (2019) Assessing water retention and correlation to climate conditions of five plant species in greywater treating green walls. *Water Research*. **167**, 115092.
- Riley, B. (2017) The state of the art of living walls: Lessons learned. *Building and Environment*. **114**, 219–232.
- Romaniak, A. (2017) Assessment of the relation between atmospheric precipitation and rainwater runoff for various urban surfaces. *Journal of Water and Land Development*. **32**(1), 87–94.
- Rossman, L.A., Huber, W.C. (2016) Storm Water Management Model Reference Manual Volume III – Water Quality. *U.S. Environmental Protection Agency*. **III**(July), 231.
- Rozos, E., Makropoulos, C., Maksimović, Č. (2013) Rethinking urban areas: an example of an integrated blue-green approach. *Water Science and Technology: Water Supply*. **13**(6), 1534–1542.
- Sánchez-Reséndiz, J.A., Ruiz-García, L., Olivieri, F., Ventura-Ramos, E. (2018) Experimental assessment of the thermal behavior of a living wall system in semi-arid environments of central Mexico. *Energy and Buildings*. **174**, 31–43.
- Savabi, M.R., Williams, J.R. (1995) *Evaporation and Environment, WEPP Model Documentation*. USDA-ARS National Soil Erosion Research Laboratory Publication.
- Scharf, B., Pitha, U. (2014) *Unveröffentlichte Ergebnisse aus dem Projekt 'Progreencity', Universität für Bodenkultur Wien, Institut für Ingenieurbiologie und Landschaftsbau, Arbeitsgruppe Vegetationstechnik*.
- Segovia-Cardozo, D.A., Rodríguez-Sinobas, L., Zubelzu, S. (2019) Living green walls: Estimation of water requirements and assessment of irrigation management. *Urban Forestry & Urban Greening*. **46**(August 2018), 126458.
- Semadeni-Davies, A., Hernebring, C., Svensson, G., Gustafsson, L.-G. (2008) The impacts of climate change and urbanisation on drainage in Helsingborg, Sweden: Suburban stormwater. *Journal of Hydrology*. **350**(1–2), 114–125.
- Senatsverwaltung für Stadtentwicklung Berlin (2007) *Innovative Wasserkonzepte Betriebswassernutzung in Gebäuden*. Berlin.
- Simperler, L., Himmelbauer, P., Stöglehner, G., Ertl, T. (2018) Siedlungswasserwirtschaftliche Strukturtypen und ihre Potenziale für die dezentrale Bewirtschaftung von Niederschlagswasser. *Österreichische Wasser- und Abfallwirtschaft*. **70**(11–12), 595–603.

## References

---

- Singh, P.K., Yaduvanshi, B.K., Patel, S., Ray, S. (2013) SCS-CN Based Quantification of Potential of Rooftop Catchments and Computation of ASRC for Rainwater Harvesting. *Water Resources Management*. **27**(7), 2001–2012.
- Sojka, S., Younos, T., Crawford, D. (2016) Modern Urban Rainwater Harvesting Systems: Design, Case Studies, and Impacts. In T. Younos & T. E. Parece, eds. *Sustainable Water Management in Urban Environments. The Handbook of Environmental Chemistry*, vol 47. Cham: Springer International Publishing Switzerland, pp. 209–234.
- Stratigea, D., Makropoulos, C. (2015) Balancing water demand reduction and rainfall runoff minimisation: modelling green roofs, rainwater harvesting and greywater reuse systems. *Water Science and Technology: Water Supply*. **15**(2), 248–255.
- Taha, H. (1997) Urban climates and heat islands: albedo, evapotranspiration, and anthropogenic heat. *Energy and Buildings*. **25**(2), 99–103.
- Technische Universität Wien, Universität für Bodenkultur Wien (2018) *Forschungsbericht Vegetationstechnische und bauphysikalischen Monitoring des 'Vertikalen Gartens' der MA31 in der Grabnergasse 4-6, 1060 Wien*.
- United Nations (2018) World Urbanization Prospects: The 2018 Revision. Key Facts. *United Nations Economic & Social Affairs*.
- Vertical Green 2.0 (2018) Project presentation. [online]. Available from: <https://jpi-urbaneurope.eu/project/vertical-green-2-0/> [Accessed December 17, 2019].
- Walsh, T.C., Pomeroy, C.A., Burian, S.J. (2014) Hydrologic modeling analysis of a passive, residential rainwater harvesting program in an urbanized, semi-arid watershed. *Journal of Hydrology*. **508**, 240–253.
- Woods Ballard, B., Wilson, S., Udale-Clarke, H., Illman, S., Scott, T., Ashley, R., Kellagher, R. (2015) *The SUDS manual*. London: CIRIA.
- Van de Wouw, P.M.F., Ros, E.J.M., Brouwers, H.J.H. (2017) Precipitation collection and evapo(transpi)ration of living wall systems: A comparative study between a panel system and a planter box system. *Building and Environment*. **126**, 221–237.
- Zluwa, I. (2019) *Personal communication*.

## 9. Appendix

### 9.1 Details VGS database

Table 7: General data and location information of the VGS investigated.

General data			Location			
ID	Measurement period	Installation	Address	Climate	Weather data	Aspect
<u>Kandl_</u> <u>Technetal*</u>	January 2016 to June 2017	2015	Vienna, Austria	Dfb	-	S
<u>Schuhmeier_</u> <u>Technetal*</u>	March to September 2018 (10 measures)	2017	Vienna, Austria	Dfb	-	-
<u>MA31</u>	March to November 2018	2015	Vienna, Austria	Dfb	-	SW
<u>Madrid_VGS</u>	March to June, 2017	2017	Madrid, Spain	Csa	Precipitation	E
<u>Planter box_</u> <u>Eindhoven</u>	November to January, 2011	2011	Eindhoven, Netherlands	Cfb	Temperature, relative humidity, global radiation, precipitation	W
<u>Melbourne_</u> <u>VGS</u>	August 2016 to February 2018	October 2015	Melbourne, Australia	Cfb	Temperature	W
<u>Kandl_</u> <u>Optigrün*</u>	January 2016 to June 2017	2015	Vienna, Austria	Dfb	-	S
<u>Diefenbach_</u> <u>Optigrün*</u>	July to September 2018 (6 measures)	2017	Vienna, Austria	Dfb	-	-
<u>Mexico_VGS</u>	2015	2015	Querétaro, Mexico	BSh	Precipitation, solar radiation, relative humidity, temperature	S
<u>Panel_</u> <u>Eindhoven</u>	November to January, 2011	2011	Eindhoven, Netherlands	Cfb	Temperature, relative humidity, global radiation, precipitation	W
<u>Site A_Berlin</u>	July and August, 2013	-	Berlin, Germany	Dfb	Incoming short-wave radiation, air temperature, relative humidity	SSW
<u>Site B_Berlin</u>	August, 2014	-	Berlin, Germany	Dfb	Incoming short-wave radiation, air temperature, relative humidity	E
<u>Site C_Berlin</u>	March to October, 2014	2013	Berlin, Germany	Dfb	Incoming short-wave radiation, outgoing long-wave radiation, wind speed, relative humidity, air temperature	W
<u>StAnna</u>	2018, 2019	-	Vienna, Austria	Dfb	-	E

Table 8: System design of the VGS investigated.

ID	System design				Substrate characteristics
	Greened area m <sup>2</sup>	Substrate volume m <sup>3</sup>	Relative substrate volume m <sup>3</sup> · m <sup>-2</sup>	Substrate composition	
<u>Kandl Techmetal*</u>	51.06	2.80	0.05	Brick chippings und compost	-
<u>Schuhmeier Techmetal*</u>	19.93	1.14	0.06	Potting soil with expanded clay	-
<u>MA31</u>	149.42	89.65	0.60	Granulite, expanded clay chippings, perlite, compost class A+	28.37 % water holding capacity
<u>Madrid VGS</u>	4.44	0.22	0.05	Mixture of blond and black peat, coconut fibre, perlite, vermiculite, earthworm humus and diatomite	221 kg.m-3 substrate bulk density, 46.89% Water holding capacity, 60.4% organic matter, 88.1% total porosity, 11.9% solid fraction
<u>Planter box Eindhoven</u>	0.33	0.04	0.11	Potting soil	High water buffering capacity
<u>Melbourne VGS</u> <u>Ophiopogon japonicus</u>	0.09	0.03	0.33	Perlite and coco coir (ratio 1:2)	-
<u>Melbourne VGS</u> <u>Carex appressa</u>	0.09	0.03	0.33	Perlite and coco coir (ratio 1:2)	-
<u>Melbourne VGS</u> <u>Nephrolepis oblitterata</u>	0.09	0.03	0.33	Perlite and coco coir (ratio 1:2)	-
<u>Melbourne VGS</u> <u>Liriope muscari</u>	0.09	0.03	0.33	Perlite and coco coir (ratio 1:2)	-
<u>Melbourne VGS</u> <u>Myoporum parvifolium</u>	0.09	0.03	0.33	Perlite and coco coir (ratio 1:2)	-
<u>Kandl Optigrün*</u>	14.40	0.86	0.06	Lava stone chippings	-
<u>Diefenbach Optigrün*</u>	9.60	0.58	0.06	Lava stone chippings	-
<u>Mexico VGS</u>	5.46	0.27	0.05	70% black peat, 17% of worm humus, 10% of coconut fibre and 3% of volcanic stone	-
<u>Panel Eindhoven</u>	0.67	0.04	0.06	Mineral wool	Low water buffering capacity
<u>Site A Berlin</u>	36	-	-	Humic sand	-
<u>Site B Berlin</u>	0.77	-	-	Grown soil	-
<u>Site C Berlin</u>	25.06	0.5	0.02	Middle-sandy coarse sand	Particle size distribution, 27-35% air capacity, 6-10% useable field capacity
<u>StAnna</u>	264	-	-	Grown soil	-



Table 9: Part 1 – Planting of the VGS investigated.

ID	Plant species	Planting					Relative biomass $\frac{g}{m^2}$
		Total plant number $\frac{number}{m^2}$	Relative plant number $\frac{number}{m^2}$	WLAI $\frac{m^2}{m^2}$	Course of greened area	Total biomass $\frac{g}{m^2}$	
<u>Kandl_Techmetal*</u>	<i>Achillea millefolium</i> , <i>Allium schoenoprasum</i> , <i>Antirrhinum majus</i> , <i>Anthemis tinctoria</i> , <i>Bergenia cordifolia</i> , <i>Calamintha nepeta</i> 'Triumphator', <i>Cymbalaria muralis</i> , ( <i>Dinthus plumarius</i> 'Greystone'), <i>Eruca sativa</i> , <i>Geranium cantabrigiense</i> 'Biokova', <i>Geranium makrorrhizum</i> , <i>Lysimachia nummularia</i> , ( <i>Origanum vulgare</i> ), ( <i>Phlox subulata</i> ), <i>Sanguisorba minor</i> , ( <i>Salvia argentea</i> ), <i>Salvia officinalis</i> , <i>Sedum floriferum</i> 'Weißenstephaner Gold', <i>Sedum reflexum</i> , <i>Sedum spurium</i> , <i>Sedum telephium</i> , ( <i>Stachys byzantina</i> 'Silver Carpet'), <i>Teucrium chamaedris</i>	1021	20	-	No	3920.34	167.90
<u>Schuhmeier_Techmetal*</u>	<i>Bergenia cordifolia</i> , <i>Bergenia cordifolia</i> 'Eroica', <i>Epimedium x perralchicum</i> 'Frohleiter', <i>Dryopteris filix-mas</i> , <i>Lamium maculatum</i> 'White Nancy', <i>Brunnera macrophylla</i> 'Looking Glass', <i>Corydalis lutea</i> , <i>Lysimachia nummularia</i> , <i>Heuchera micrantha</i> 'Miracle', <i>Heuchera x villosa</i> 'Brownie', <i>Heuchera x cultorum</i> 'Lime Marmelade', <i>Heuchera micrantha</i> 'Berry Smoothie', <i>Carex sylvatica</i> , <i>Hyacinthus</i> sp.	438	22	-	No	2222.55	233.56
<u>MA31</u>	<i>Akebia quinata</i> , <i>Aristolochia macrophylla</i> , <i>Lonicera henryi</i> , <i>Lonicera japonica</i> , <i>Lonicera telmanniana</i> , <i>Wisteria floribunda</i> , <i>Aster ageratoides</i> 'Asran', <i>Bistorta amplexicaulis</i> , <i>Calamintha nepeta</i> ssp. <i>nepeta</i> , <i>Geranium x cantabrigiense</i> , <i>Haconechloa macra</i> , <i>Hemerocallis x cultorum</i> , <i>Iris x barbata-elliator</i> 'Interpol', <i>Tradescantia andersoniana</i>	829	6	-	No	425914.12	2850.41
<u>Madrid_VGS</u>	<i>Carex oshimensis</i> , <i>Jacobaea maritima</i> , <i>Cyrtomitium falcatum</i> , <i>Lampranthus spectabilis</i> , <i>Luzula nivea</i> , <i>Tulbaghia violacea</i> , <i>Vinca minor</i>	168	38	-	Yes	-	-
<u>Planter box_Eindhoven</u>	No specification	-	-	-	Yes	-	-
<u>Melbourne_VGS</u> <u><i>Ophiopogon japonicus</i></u>	<i>Ophiopogon japonicus</i>	5	56	-	Yes	-	-
<u>Melbourne_VGS</u> <u><i>Carex appressa</i></u>	<i>Carex appressa</i>	5	56	-	Yes	-	-
<u>Melbourne_VGS</u> <u><i>Nephrolepis oblitterata</i></u>	<i>Nephrolepis oblitterata</i>	5	56	-	Yes	-	-
<u>Melbourne_VGS</u> <u><i>Liriope muscari</i></u>	<i>Liriope muscari</i>	5	56	-	Yes	-	-
<u>Melbourne_VGS</u> <u><i>Myoporum parvifolium</i></u>	<i>Myoporum parvifolium</i>	5	56	-	Yes	-	-

Table 10: Part 2 – Planting of the VGS investigated.

ID	Plant species	Planting					
		Total plant number number	Relative plant number number · m <sup>-2</sup>	WLAI m <sup>2</sup> · m <sup>-2</sup>	Course of greened area	Total biomass g	Relative biomass g · m <sup>-2</sup>
<u>Kandl Optigrün*</u>	<i>Ajuga reptans</i> , <i>Allium schoenoprasum</i> , <i>Bergenia cordifolia</i> , ( <i>Bistorta amplexicaulis</i> ), <i>Campanula portenschlagiana</i> - <i>Dalmatiner</i> , <i>Geranium macrorrhizum</i> , <i>Geranium renardii</i> , <i>Geranium sanguineum</i> , <i>Heuchera micrantha</i> 'Palace Purple', <i>Heuchera sanguinea</i> , <i>Heuchera x Pink Lady</i> , ( <i>Lysimachia nummularia</i> ), <i>Nepeta x fassenii</i> , <i>Phlox subulata</i> <i>Atropupurea</i> , <i>Saponaria</i> sp., <i>Sedum album</i> , <i>Sedum floriferum</i> , <i>Sedum hybridum</i> , <i>Sedum reflexum</i> , <i>Sedum spurium</i> , <i>Sedum telephium</i>	432	30	-	No	1235.57	85.80
<u>Diefenbach Optigrün*</u>	<i>Aster dumosus</i> 'Kassel', <i>Bergenia cordifolia</i> , <i>Campanula portenschlagiana</i> , <i>Fragaria vesca</i> var. <i>Vesca</i> , <i>Gaura lindheimeri</i> , <i>Geranium macrorrhizum</i> , <i>Helianthemum x cultorum</i> 'Bronzeteeppich', <i>Helianthemum x cultorum</i> 'Golden Queen', <i>Hemerocallis Hybride</i> 'Stella de Oro', <i>Heuchera micrantha</i> 'Palace Purple', <i>Heuchera sanguinea</i> <i>Leuchtkäfer</i> , <i>Phlox subulata</i> , <i>Phlox subulata</i> 'White Delight', <i>Potentilla heumanniana</i> , <i>Sedum floriferum</i> 'Weihenstephaner Gold', <i>Sedum pachyclados</i> , <i>Sedum telephium</i> 'Herbstfreude'	288	30	-	No	947.27	98.67
<u>Mexico VGS</u>	<i>Sedum obtusifolium</i> , <i>Sedum reflexum</i> , <i>Sedum crassulaceae</i> , <i>Sedum mexicanum</i> , <i>Tall fescue</i> , <i>Sedum moranense</i> , <i>Chlorophytum comosum</i> , <i>Hedera helix</i>	660	121	-	No	-	-
<u>Panel Eindhoven</u>	No specification	-	-	-	Yes	-	-
<u>Site A Berlin</u>	<i>Parthenocissus tricuspidata</i>	1	-	1.9	Yes	-	-
<u>Site B Berlin</u>	<i>Hedera helix</i>	1	-	3	Yes	-	-
<u>Site C Berlin</u>	<i>Fallopia baldschuanica</i>	1	-	3	Yes	-	-
<u>StAnna</u>	<i>Hedera helix</i> , <i>Wisteria floribunda</i> , <i>Parthenocissus quinquefolia</i> , <i>Lonicera</i> sp., <i>Hydrangea</i> sp.	-	-	-	No	-	-

Table 11: Part 1 – Water supply of the VGS investigated.

ID	Water supply						Provided water balance components
	Irrigation system	Water source	Dosing regularity	Dosing time $\frac{\text{min. dosing}^{-1}}{\text{min. dosing}^{-1}}$	Dosing volume $\frac{\text{l. day}^{-1}}{\text{l. day}^{-1}}$	Annual water/irrigation $\frac{\text{m}^3}{\text{m}^3}$	
<u>Kandl Technetal*</u>	Drip irrigation	Tap water	Winter: Mon, Fri Summer: Mon-Sun	3	-	14.31	-
<u>Schuhmeier Technetal*</u>	Drip irrigation <3°C frost monitoring	Tap water	Oktober-March: Mon, Thu May-September: Mon, Wed, Sat	3	-	7.35	-
<u>MA31</u>	Drip irrigation Sensor controlled	Tap water	Winter: irrigation if 50% of max. water content Summer: irrigation if 60% of max. water content	-	-	74.71	ET
<u>Madrid VGS</u>	Drip irrigation	Tap water	Set by maintenance staff to saturate the substrate	1, 2 or 3 min each day	-	4.17	ET
<u>Planter box Eindhoven</u>	Drip irrigation	Rainwater, tap water	only once during measurement period with 1430 ml	-	-	0.12	Precipitation, ET, water balance flow chart with all components in percent
<u>Melbourne VGS</u> <u>Ophiopogon japonicus</u>	Drip irrigation Water reused from drainage	Synthetic light greywater mix, potable water	Mon-Fri	30	-	0.026	Evaporation (monthly min and max values), transpiration for 5 different plant types (monthly min and max values)
<u>Melbourne VGS</u> <u>Carex appressa</u>						0.058	
<u>Melbourne VGS</u> <u>Nephrolepis oblitterata</u>						0.056	
<u>Melbourne VGS</u> <u>Liriope muscari</u>						0.040	
<u>Melbourne VGS</u> <u>Myoporum parvifolium</u>						0.044	
<u>Kandl Optigrün*</u>	Drip irrigation	Tap water	Winter: Mon-Sun, 2x per day Spring, autumn: Mon-Sun, 6x per day Summer: Mon-Sun, 6x per day	3 3 5	-	10.78	-
<u>Diefenbach Optigrün*</u>	Drip irrigation	Tap water	All year: Mon-Sun	30	-	5.61	-

Table 12: Part 2 – Water supply of the VGS investigated.

ID	Water supply						Provided water balance components
	Irrigation system	Water source	Dosing regularity	Dosing time $\frac{\text{min. dosing}^{-1}}{\text{min. dosing}^{-1}}$	Dosing volume $\frac{\text{l. day}^{-1}}{\text{l. day}^{-1}}$	Annual water/irrigation $\frac{\text{m}^3}{\text{m}^3}$	
<u>Mexico VGS</u>	Drip irrigation Sensor controlled	Rainwater Tap water	No interval given	-	-	33.56	-
<u>Panel Eindhoven</u>	Drip irrigation	Rainwater Tap water	Every 3 h	1	0.79	0.42	Precipitation, ET, water balance flow chart with all components in percent
<u>Site A Berlin</u>	No specification	Rainwater Tap water	Irregular	-	-	-	Transpiration
<u>Site B Berlin</u>	Only run-on	Rainwater Tap water	-	-	-	-	Transpiration
<u>Site C Berlin</u>	Constant standing water table in 0.45m depth	Tap water	-	-	-	-	Evaporation, Transpiration
<u>StAnna</u>	Drip irrigation Sensor controlled	Tap water	No interval given	-	-	36.69	-

## 9.2 Water demand and irrigation amounts

Table 13: Water demand and irrigation amounts (\*) per month ( $\text{m}^3 \cdot \text{month}^{-1}$ ) and annual sum ( $\text{m}^3 \cdot \text{year}^{-1}$ ).

ID	January	February	March	April	May	June	July	August	September	October	November	December	Sum
<u>Kandl_Techmetal*</u>	0.044	0.076	0.725	1.396	1.127	2.340	2.250	1.857	2.351	1.653	0.367	0.124	14.308
<u>Schuhmeier_Techmetal*</u>	-	-	0.154	0.511	0.682	0.750	0.984	1.016	0.127	-	-	-	7.345
<u>MA31</u>	-	-	0.510	2.900	7.170	12.740	14.610	18.020	9.380	7.650	1.730	-	74.710
<u>Madrid_VGS</u>	0.069	0.099	0.248	0.293	0.523	0.733	0.757	0.771	0.400	0.138	0.107	0.030	4.167
<u>Planter box Eindhoven</u>	0.005	0.005	0.007	0.011	0.014	0.015	0.016	0.014	0.012	0.008	0.006	0.004	0.119
<u>Melbourne_VGS</u>	0.003	0.003	0.003	0.002	0.002	0.001	0.001	0.002	0.002	0.002	0.002	0.003	0.026
<u>Ophiopogon japonicus</u>													
<u>Melbourne_VGS</u>	0.007	0.007	0.007	0.005	0.004	0.003	0.003	0.003	0.004	0.005	0.006	0.007	0.058
<u>Carex appressa</u>													
<u>Melbourne_VGS</u>	0.007	0.007	0.007	0.005	0.003	0.002	0.002	0.003	0.003	0.005	0.005	0.007	0.056
<u>Nephrolepis oblitterata</u>													
<u>Melbourne_VGS</u>	0.005	0.005	0.005	0.003	0.003	0.002	0.002	0.002	0.002	0.003	0.004	0.005	0.040
<u>Liriope muscari</u>													
<u>Melbourne_VGS</u>	0.006	0.005	0.005	0.003	0.003	0.002	0.002	0.002	0.003	0.004	0.004	0.005	0.044
<u>Myoporum parvifolium</u>													
<u>Kandl_Optigrün*</u>	0.000	0.171	0.439	1.083	1.066	1.470	1.723	1.353	1.800	1.323	0.353	0.000	10.779
<u>Diefenbach_Optigrün*</u>	-	-	-	-	-	-	0.213	1.385	0.235	-	-	-	5.612
<u>Mexico_VGS</u>	1.240	1.120	1.860	3.000	4.960	4.800	4.340	3.720	3.000	2.480	1.800	1.240	33.560
<u>Panel Eindhoven</u>	0.015	0.017	0.025	0.036	0.052	0.058	0.060	0.056	0.042	0.029	0.018	0.012	0.421
<u>Site A Berlin</u>	-	-	-	-	-	-	1.487	1.401	-	-	-	-	-
<u>Site B Berlin</u>	-	-	-	-	-	-	-	0.021	-	-	-	-	-
<u>Site C Berlin</u>	-	-	0.057	0.436	0.639	0.727	1.027	1.172	0.666	0.505	-	-	-
<u>StAnna</u>	-	-	-	-	-	-	-	-	-	-	-	-	36.692

## 10. Curriculum Vitae

### Flora Prenner, BSc

#### Personal data

---

Data of birth	20.01.1994
Place of birth	Vienna, Austria
Nationality	Austria
E-mail	flora.prenner@hotmail.com
Telephone	0043 699 1828 3989



#### Education

---

2017 – 2020	<b>Master of Science</b> Water Management and Environmental Engineering University of Natural Resources and Applied Life Sciences, Vienna
2019	<b>Summer school</b> Nature-based solutions for the management of rural-urban landscapes Malta College of Arts, Science & Technology
2015	<b>Erasmus exchange</b> Water Science and Technology Ecole polytechnique universitaire de Montpellier, France
2012 – 2016	<b>Bachelor of Science</b> Environment and Bio-resource Management University of Natural Resources and Applied Life Sciences, Vienna
2004 – 2012	<b>High school</b> Graduated with honours from Gymnasium Perchtoldsdorf, Lower Austria

#### Work Experience

---

03/2019 – 06/2019	<b>University of Natural Resources and Applied Life Sciences, Vienna</b> Tutor “Planning and Design in Water Supply and Wastewater Treatment”
07/2017 – 08/2017	<b>Hinker+Binder ZT GmbH, Brunn am Gebirge</b> Project assistance (Flood protection, sewage systems, drainage)
07/2016	<b>Österreichische Hagelversicherung VVaG, Vienna</b> Customer service and handling of damage compensations

## Curriculum Vitae

---

- 09/2015 – 11/2015 **Institute of Social Ecology University of Klagenfurt**, Vienna  
Academic assistance  
Research on CO<sub>2</sub> emission and reduction targets in Austria
- 03/2014 – 06/2014 **University of Natural Resources and Applied Life Sciences**, Vienna  
Tutor “Environment and Resource Economics”
- 08/2013 **Esterházy Forest and Nature Management**, Eisenstadt  
Assistance in forest management, cultivation and organisation of logging

## Additional experience

---

- 08/2018 – 09/2018 **Voluntary work with CLAC/Fairtrade**, Costa Rica and El Salvador  
Generation of commercial profiles of certified cooperatives
- 10/2017 – today **Voluntary work with study representatives of Environmental and Civil Engineering**, Vienna  
Organisation of events, excursions and tutorials
- 08/2012 **Institute of Social Ecology University of Klagenfurt**, Vienna  
Participation in project Rio+20 Jugendliche ziehen Bilanz  
Literature research population growth, diet and bioenergy

## Skills and Hobbies

---

Languages	German	Native
	English	C1 – Proficient
	French	B2 – Intermediate
	Spanish	A2 – Basic
Software	Microsoft Office	Advanced
	AutoCAD	Advanced
	ArcGIS	Intermediate
	R (Programming)	Basic
	EPANET	Intermediate
Driving licence	Class B	
Hobbies	Sports (Climbing, cycling, hiking)	
	Creative work (Drawing, painting, cooking)	
	Travelling	

## **11. Affirmation**

I certify, that the master thesis was written by me, not using sources and tools other than quoted and without use of any other illegitimate support.

Furthermore, I confirm that I have not submitted this master thesis either nationally or internationally in any form.

*Vienna, February 11th, 2020, Flora Prenner*